Opposite trends of sea-breeze speeds and gusts in Eastern Spain, 1961-2019

Shalenys Bedoya-Valestt (shalevale@gmail.com)
Spanish National Research Council: Consejo Superior de Investigaciones Cientificas
https://orcid.org/0000-0001-7386-9127
Cesar Azorin-Molina
Spanish National Research Council: Consejo Superior de Investigaciones Cientificas
Luis Gimeno
University of Vigo: Universidade de Vigo
Jose A. Guijarro
Spanish State Meteorological Agency: Agencia Estatal de Meteorologia
Victor J. Sanchez-Morcillo
Polytechnic University of Valencia: Universitat Politecnica de Valencia
Enric Aguilar
Rovira i Virgili University: Universitat Rovira i Virgili
Manola Brunet
Rovira i Virgili University: Universitat Rovira i Virgili

Research Article

Keywords: sea breeze, Mediterranean, Iberian Peninsula, wind, trends, variability

Posted Date: March 30th, 2022

DOI: https://doi.org/10.21203/rs.3.rs-1450729/v1

Abstract

Most studies on wind variability have deepen into the *stilling vs. reversal* phenomena at global to regional scales, while the long-term changes in local-scale winds such as sea-breezes (SB) represent a gap of knowledge in climate research. The state-of-the-art of the wind variability studies suggests a hypothetical reinforcement of SB at coastal stations. We first developed a robust automated method for the identification of SB days. Then, by using homogenized wind observations from 16 stations across Eastern Spain, we identified 9,312 episodes for analyzing the multidecadal variability and trends in SB speeds, gusts and occurrence for 1961-2019. The major finding is the opposite trends and decoupled variability of SB speeds and gusts: the SB speeds declined significantly in all seasons (except for winter), and the SB gusts strengthened at the annual scale and in autumn-winter, being most significant in autumn. Our results also show that the SB occurrence has increased across most of Eastern Spain, although presenting contrasting seasonal trends: positive in winter and negative in summer. We found that more frequent anticyclonic conditions, NAOI+ and MOI+ are positively linked to the increased winter occurrence; however, the causes behind the opposite trends in SB speeds and gusts remain unclear. The SB changes are complex to explain, involving both large-scale circulation and physical-local factors that challenge the understanding of the opposite trends. Further investigation is needed to assess whether these trends are a widespread phenomenon, while climate models could simulate the drivers behind these decoupled SB changes in a warmer climate.

1 Introduction

From a global perspective, open-ocean and coastal winds are blowing harder in the Southern Hemisphere (Young and Ribal 2019) and in upwelling systems (Sydeman et al. 2014), whereas terrestrial *stilling* (i.e., decline in surface winds until the 2010s; Roderick et al. 2007) is expected to continue throughout the present century across mid-to-high latitudes of the Northern Hemisphere (Deng et al. 2021; Zha et al. 2021), despite of the *reversal* observed in the last decade (Zeng et al. 2019). Among the possible causes discussed for the atmospheric *stilling* and *reversal* phenomena (Wu et al. 2018), changes in land-use and surface roughness (Vautard et al. 2010) and the internal decadal ocean-atmosphere oscillations (Zeng et al. 2019; Deng et al. 2021) are the most likely drivers. However, besides the interhemispheric asymmetry of surface wind changes, these are changing differently in sign and magnitude at seasonal-scale (Azorin-Molina et al. 2021), latitudinal-scale (Zhang et al. 2020; Zha et al. 2021), and depending on the locations, i.e., differences between coastal, inland and mountain stations (Minola et al. 2016; Azorin-Molina et al. 2018a). For example, increased trends in summer-coastal winds have been observed around the world (Azorin-Molina et al. 2014a; Kim and Paik 2015; Azorin-Molina et al. 2016, 2018a; Zhang et al. 2020), and most of these authors point out that a reinforcement in local circulations (i.e., sea-breeze, hereafter SB) could be driving these trends, as SB represent the dominant local wind in most coastal regions of the world (Simpson, 1994). Nevertheless, the mechanisms behind seasonal and local-based wind speed trends remain largely unknown as the *stilling vs. reversal* research has not yet quantified changes

according to the types of winds; e.g., westerlies, trade winds, local winds, etc (Azorin-Molina et al. 2018b). This study covers the research niche of assessing changes and multidecadal variability in SB.

Despite being a widely studied phenomenon through numerical simulations (Drobinski et al. 2018), cases-study (Cana et al. 2020), and short-term climatology (Azorin-Molina et al. 2011a; El-Geziry et al. 2021), the research on long-term SB changes has been limited because of the short length, low spatial and temporal resolution and unreliability of observations over the land and ocean surfaces. To date, few studies have addressed more than a decade of SB climate (Redaño et al. 1991; Laird et al. 2001; Masselink and Pattiaratchi 2001; Zhu and Atkinson 2004; Alomar and Grimalt 2008; Misra et al. 2011; Steele et al. 2015; Perez and Silva Dias 2017; Khan et al. 2018; Guedje et al. 2019; Coulibaly et al. 2019; Hwang et al. 2020; Grau et al. 2021; Shen et al. 2021a), and only five recent studies have focused on analyzing their long-term trends and multidecadal variability (Shen et al. 2019; Pazandeh-Masouleh et al. 2019; Shen and Zhao 2020, Shen et al. 2021a, 2021b). In fact, there is no study examining how changes in SB influence the seasonal trends and variability of winds. The recent state-of-the-art of the SB trend estimates over the globe is not conclusive, with strong suggestions to the key role of local mechanisms. For example, the dynamic factors (i.e., increasing surface roughness and urbanization expansion) have primarily driven the slowdown of summer SB speed (-0.033 m s^{-1} $decade^{-1}$) in Shanghai (China) for 1994–2014 (Shen et al. 2019); and also in Colombo (Sri Lanka) for the same period, with a greater wind speed decline after 2010 (Shen et al. 2021b). On the opposite, the increase in air temperature has driven an annual and seasonal strengthening of the maximum SB speed in Adelaide (Australia) for 1955–2007 (Pazandeh-Masouleh et al. 2019), and recent studies evidence ongoing positive wind trends in Adelaide and Perth for 1994–2014 (Shen et al. 2021b). In addition, solar radiation also determined winter variations on SB speed in Los Angeles (USA) for 1994–2014 (Shen et al. 2021a). In the Mediterranean area, where climate conditions favor the development of SB, trends vary locally, e.g., Thyna (Tunez) and Tel Aviv (Israel) present no significant variations for 1994–2014, Rome (Italy) shows positive trends and Barcelona (Spain) negative ones for the same period (Shen et al. 2021b). These discrepancies evidence that SB changes are location-based, due to the different coastline orientation and complex terrain (Qian et al. 2012), land-use changes (Kusaka et al. 2000), large-scale atmospheric circulation (Arritt 1993), air-surface temperature rise (Lebassi-Habtezion et al. 2011) or ocean-atmosphere oscillations (Azorin-Molina and Lopez-Bustins 2008) to mention a few, which can interact each other at once and control the SB features (Miller et al. 2003), thereby challenging the understanding of their changes and variability.

Focusing on the Iberian Peninsula, Azorin-Molina et al. (2014a, 2016) reported positive trends of wind speed and gusts in the warm semester (May-October), which might be associated with a strengthening of local wind circulations; e.g., meanwhile Jerez et at. (2012) pointed out a possible reinforcement of local winds due to the soil moisture depletion and the enhancement of the Iberian thermal low. However, it is still unknown how local SB has reacted to the mix of local and regional feedbacks and a warming climate. Therefore, it is of huge scientific interest deepening in the knowledge of SB long-term trends in the framework of the *stilling vs. reversal* phenomena. The multidecadal research of SB is necessary, as these winds have a large impact on broad socioeconomic and environmental spheres (Simpson, 1994).

By bringing moisture to coastal and continental areas from ocean basins (Drobinski et al. 2018; Davis et al. 2019), SB affect evapotranspiration and precipitation processes (Azorin-Molina et al. 2009; Azorin-Molina et al. 2015) with direct implications over agriculture, hydrology and local weather and climate (Mahrer and Rytwo 1991; Simpson 1994; Zhu et al. 2017; Pausas and Millán 2019). Besides, changes on SB speed can also may alter the efficiency of wind power industry during peak demand periods (Steele et al. 2015). Moreover, these onshore winds greatly affect air quality and human health, by transporting air pollutants from coastal areas toward inland cities (Papanastasiou et al. 2010; Bei et al. 2018). Thus, a better understanding of changes in SB in a warming climate could support stakeholders and policy-makers to adapt to future wind projections.

The aim of this study is to analyze for the first time the long-term trends, multidecadal variability and possible drivers of the near-surface wind speed changes (mean and gusts) on days dominated by SB circulations in Eastern Spain for 1961–2019. The specific objectives of this study are (i) to develop a robust and automatic selection approach for creating the first long-term SB database from reliable, reconstructed and homogenized wind series; (ii) to advance in the study of the seasonal changes in the *stilling-reversal* phenomena from a wind type (i.e., SB circulations) perspective and for both mean and gust speeds; and (iii) to improve the understanding of the causes of SB variability and trends in a warming climate.

2 Data And Methods

2.1 Study region

We define Eastern Spain as the area comprising the Mediterranean coast of Spain between 36° – 41°N and 4.5°W – 4.5°E (Fig. 1), characterized by a complex topography: i.e., coastal plains, deltas, river mouths and valleys, flanked by inland mountain ranges such as the Betic, Prebetic and Iberian systems. The study area covers 82,165 km^2 of territory and 3,017 km of coastline (from Malaga to Barcelona, including the Balearic Islands), and it is located in the Western Mediterranean basin. The climate is typically Mediterranean with mild winters and dry hot summers, modulated by the cooling effect of the SB, which represent the most dominant wind circulation at summertime (Olcina-Cantos and Azorin-Molina 2004). Because stable atmospheric conditions (i.e., high insolation and weak surface pressure gradient) are frequent throughout the year, SB can develop even during the cold semester (November-April), occurring in 2/3 of the days in the year (Azorin-Molina and Martín-Vide 2007). In addition, this local wind circulation can penetrate ~ 150 km inland (Kottmeier et al. 2000) through river valleys (Simpson et al. 1977; Arritt 1993), being responsible for most convection (Azorin-Molina et al. 2009) and summer precipitation (Azorin-Molina et al. 2014b) in mountainous areas inland.

We split the Eastern Spain into five regions according to the orientation of the coastline, which strongly influences SB dominant direction (Azorin-Molina and Lopez-Bustins 2008; see Fig. 1): (i) the Southern coast (coastline oriented from W to E) on the Betic system, with the highest mountain range peak (Mulhacén, 3,478.6 m a.s.l); (ii) the South-eastern coast (SW to NE) on the Prebetic system and irregular

coastal relief (mostly headlands and cliffs); (iii) the Eastern coast (S to N) with the Iberian mountain range at west, large coastal plains at the coast, and the most important delta of the region: Ebro delta; (iv) the North-eastern coast (SW to NE) on the Catalan coastal range; and (v) the Balearic Islands (W to E), a group of islands with quite complex orography (altitudes reach 1,445 m a.s.l in the Serra de Tramuntana mountain range).

(Fig. 1 about here)

2.2 Observed wind speed data

Our dataset, including wind speed observations (daily mean and daily maximum wind gusts; in m s^{-1}) from 16 stations located over the Eastern Spain (see Fig. 1) for 1961–2019 represents the longest climatological SB study in the region. The Spanish Meteorological Agency (AEMET) provided the wind speed data, measured at standard 10 m height with different types of anemometers as detailed in Azorin-Molina et al. (2014a). We computed the daily averages from sub-daily observations at 0700, 1300, and 1800 UTC, discarding the nighttime one (i.e., 0000 UTC) where the breeze flow reverses, giving rise to the land-breeze. We selected those existing meteorological stations where the distance to the coastline does not exceed 20 km (given in Table 1), because the inland penetration of SB could be reduced in wintertime or inhibited by offshore synoptic flows (Salvador and Millán 2003; Azorin-Molina and Chen 2009; Azorin-Molina et al. 2011a). Five of the selected stations are sited in urban environments (see Table 1), while the rest are located in well exposed sites at airports, reducing the frequency of potential inhomogeneities due to surrounding changes in urbanization (Azorin-Molina et al. 2014a).

Table 1
Description of the meteorological stations with homogeneous wind speed measurements over the Eastern Spain (for locations see Fig. 1) for 1961–2019. In bold are shown the relocated stations used in this study. Weather stations sited in urban environments are marked with an *.

Nº	Id	Station	Lat. (Decimal º)	Long. (Decimal º)	Elevat. a.s.l. (m.)	Dist. Coast (km)	Orient. (Decimal º)	Period
1	6155A	Málaga airport *	36.67	-4.48	5	1.9	255–75	1961–2019
2	6325O	Almería airport	36.85	-2.36	21	1	255–75	1968–2019
3	7031	San Javier airport	37.79	-0.80	4	4.5	223 – 43	1961–2019
4	8019	Alicante airport	38.28	-0.57	43	4.4	223 – 43	1961–2019
5	8025	Alicante Ciudad Jardín *	38.37	-0.49	81	2.8	223 – 43	1961–2019
6	8414A	Valencia airport	39.48	-0.47	56	12.7	193 – 13	1961–2019
7	8416	Valencia Viveros *	39.48	-0.36	11	3.2	193 – 13	1961–2019
8	8500A	Castellón-Almassora *	39.96	-0.07	43	6.7	193 – 13	1976–2019
9	9981A	Tortosa	40.82	0.49	50	18	193 – 13	1961–2019
10	0016A	Reus airport	41.15	1.16	71	7.5	229 – 49	1961–2019
11	0076	Barcelona airport	41.29	2.07	4	1.5	229 – 49	1961–2019
12	0200E	Barcelona Fabra	41.42	2.12	408	8	229 – 49	1961–2019
13	B893	Menorca airport	39.85	4.22	91	3	270 – 90	1965–2019
14	B278	Palma Mallorca airport	39.56	2.74	8	3.7	270 – 90	1972–2019
15	B228	Palma Mallorca port*	39.56	2.63	3	0	270 – 90	1978–2019

Nº	Id	Station	Lat. (Decimal º)	Long. (Decimal º)	Elevat. a.s.l. (m.)	Dist. Coast (km)	Orient. (Decimal º)	Period
16	B954	Ibiza airport	38.88	1.38	6	2.8	270 – 90	1961–2019

2.3 Homogenization of wind speed data

Wind speed series were created by applying a robust quality control and homogenization protocol, following the method used by Azorin-Molina et al. (2019). Reconstructions of wind speed series were made by checking for discontinuities, due to the installation of automatic weather stations (after the 1980s) and relocation (see Table 1). All stations were homogenized to avoid disturbances in climate trends due to non-climatic break-points in wind series. Although Azorin-Molina et al. (2014a) suggest the use of some regional climate models (i.e., MM5) as reference series for homogenization due to their reliability to reproduce mesoscale circulations (such as SB), we rather used wind speed data from the National Center for Environmental Prediction-National Center for Atmospheric Research (NCEP-NCAR) reanalysis (https://psl.noaa.gov/data/gridded/data.ncep.reanalysis.html; last accessed February 24, 2022), as it covers the entire study period. Moreover, high correlated ($r = 0.4$, $p < 0.05$; up to 25 km) neighboring stations were also used to detect inhomogeneities, according to Azorin-Molina et al. (2014a). We applied the CLIMATOL package (http://www.climatol.eu/, last accessed February 24, 2022), which implements a variation of the Alexandersson's Standard Normal Homogeneity Test (SNHT; Alexandersson 1986) in all 16 stations on a daily basis, which represent one of the most used tests to detect inhomogeneities in climate series. In summary, the procedure did not detect any clearly outlier value, but corrected 68 and 76 break-points with SNHT > 25 for SB speeds and gusts respectively.

2.4 Identification and validation of sea breeze days

SB selection algorithms consist in detecting past events from well-defined criteria, such as certain thresholds for wind or thermal contrast between land-sea air (ΔT), among many others. However, there is no universal method to accurately detect SB days. Instead, SB identification depends mostly on the criteria used in each study site, physical complexity of the area and data availability (see Table 1 in Azorin-Molina et al. 2011b). In general, there is a global lack of historical observed data for many essential variables to automatically detect SB events from long-term climate series. Most historical observed data presents (i) large gaps; (ii) low quality; and (iii) limited temporal resolution to create with reliability a historical and high-quality SB database. Even when procedures such as quality control, missing data infilling, reconstruction and homogenization can be applied to entire datasets (i.e., essential climate variables for SB detection) on a sub-daily basis (Guijarro 2018; Curci et al. 2021), this implies huge computational cost and effort. To address the need to improve the processing time and accuracy in SB selection methods for long-term studies, we propose a robust automated method to identify potential SB days using alternative variables (e.g., Laird et al. 2001; Azorin-Molina and Lopez-Bustins 2008), which can be used worldwide at any coastal region with few adjustments.

The automated selection algorithm presented here is based on six alternative filters, classified in (a) synoptic and (b) local-scale conditions (see Fig. 2). The first main group (filters 1 to 3) employs the synoptic flow regime at 850 hPa (in terms of regional teleconnection patterns, synoptic weather types and geostrophic winds) as alternative criteria to reject days with large-scale synoptic disturbances for developing SB. The second group (filters 4 to 6) uses objective criteria in local weather to confirm SB passage (by onshore winds and weak wind gusts), and to ensure pure SB events (days without precipitation). After running the data through these filters, we identified 9,312 potential SB days at the regional level across Eastern Spain (Fig. 3) and between 6,741 and 8,315 SB days at the coastal level (Table 2) for 1961–2019. We distinguished between SB days at station level (i.e., exact number of events identified for each weather station), coastal level (i.e., encompass all the SB episodes presented in one same coast-region) and regional level (all SB days identified for all stations).

(Fig. 2 about here)

Table 2
SB days identified for each weather station and sub-regional coast for 1961–2019. SB days at station level means the exact number of days identified for each weather station, while days at coastal level encompass all the episodes occurred in one region.

Nº	Id	Station	Sea breeze days at station level	Coast	Sea-breeze days at coastal level
1	6155A	Málaga airport	7,457	Southern	8,315
2	6325O	Almería airport	6,271		
3	7031	San Javier airport	6,822	South-eastern	8,090
4	8019	Alicante airport	7,005		
5	8025	Alicante Ciudad Jardín	7,547		
6	8414A	Valencia airport	6,394	Eastern	8,209
7	8416	Valencia Viveros	6,520		
8	8500A	Castellón-Almassora	6,849		
9	9981A	Tortosa	4,356		
10	0016A	Reus airport	4,811	North-eastern	7,179
11	0076	Barcelona airport	6,180		
12	0200E	Barcelona Fabra	5,934		
13	B893	Menorca airport	2,959	Balearic Islands	6,741
14	B278	Palma Mallorca airport	5,642		
15	B228	Palma Mallorca port	5,783		
16	B954	Ibiza airport	5,199		

A validation is presented below, whereas thresholds and descriptions of each criterion are described as follows:

Filter 1: To assure a surface pressure gradient weak enough to develop local winds, we used the neutral phase (interval range between − 1 and 1) of the Western Mediterranean Oscillation Index (WeMOI, details in section 2.6). Azorin-Molina and Lopez-Bustins (2008) proposed it as the first criterion to detect potential SB passages associated with weak surface pressure conditions over the Western Mediterranean basin.

Filter 2: Eight weather types (A, E, NE, AE, ANE, C, N, and SE) were filtered from the automated classification by the Jenkinson and Collison´s method (1977; JC), as favorable synoptic conditions for SB (Azorin-Molina et al., 2011a). The method uses daily air pressure from NCEP-NCAR reanalysis to compute the 27 weather types defined by Lamb (1950) for the British Islands. A detailed description of the method can be found in Azorin-Molina et al. (2011a).

Filter 3: Weak geostrophic winds ($\leq$ 12 m s^{-1}) exclude days dominated by moderate-strong synoptic flows, which disturb SB development (Ramis and Alonso 1988). We calculated the daily 850 hPa geostrophic wind (in m s^{-1}) at 1200 UTC in terms of geopotential, which assumes a horizontal constant pressure gradient. Geopotential data were taken from ERA5 reanalysis dataset (available online at https://cds.climate.copernicus.eu/; last accessed February 24, 2022).

Filter 4: Winds from the sea were selected based on the coast orientation (see section 2.1 and Fig. 1) and the wind direction at 1200 UTC. Further, to include sideshore SB, we extended orientations at Table 1 in ± 15°. As some recent studies suggest the good representation of near-surface winds provided by ERA5 (Ramon et al. 2019; Minola et al. 2020), we used 10-m height zonal (u) and meridional (v) wind components at 1200 UTC to compute the wind direction.

Filter 5: Daily wind gusts $\leq$ 13.9 m s^{-1} were required to exclude moderate-strong onshore flows, as SB gusts in this region do not exceed 14 m s^{-1} (Azorin-Molina et al. 2011b). For this filter, daily observations were provided by AEMET in section 2.2.

Filter 6: Daily total precipitation < 0.1 mm d^{-1} was needed to reject days with atmospheric instability (Arillaga et al. 2020; Grau et al. 2021). Daily precipitation series were provided by AEMET for each station described in Table 1. Further, we used daily total precipitation from ERA5 to full length (since 1961) of the shortest observed-precipitation series (see Table 1) plus few missing data therein.

We evaluated the accuracy of the proposed method (PM) in this study with a reference manual method (RM) developed by Azorin-Molina et al. (2011b) in Alicante (Spain) for 2000–2005. Comparisons between databases were made by computing probabilities of detection of potential SB and non-SB episodes (NSB) first described in Laird et al. (2001), and used by Azorin-Molina et al. (2011b). Probabilities of potential detection of SB days were calculated as follows: (i) identical SB days; (ii) identical NSB days; (iii) different SB days; and (iv) different NSB days; for more details see Table S1. Our PM identified 804 SB events for Alicante Ciudad Jardín weather station (Table 3) for 2000–2005, which is more than half of the number of SB days (1,414) detected by the RM. From 37% of episodes identified for 2000–2005, the validation results for equal SB (48%) and NSB (47%) detections suggest that our method is capable to create a robust long “potential” SB database by taking only pure SB days, i.e., discarding most situations in which SB is combined with synoptic winds. Overall, the methods differed from each other in 11% SB days while 89% of NSB days are due to differences in the type of method (i.e., manual or automatic detection), test criteria, and data sources (Table 3).

(Fig. 3. about here)

Table 3
Comparison of sea-breeze (SB) and non-sea-breeze (NSB) days detected by the reference method (RM) and ours (PM) in the Alicante Ciudad Jardín station for 2000–2005. Below are described the probabilities of occurrence of SB and NSB days between PM and RM. Probabilities range from 0 to 1, where 1 indicates the equal or different detections of SB episodes. Details of the calculation are described in Table S1.

Sea-breeze days (2000–2005)			
SB day (PM)	**SB day (RM)**	**NSB day (PM)**	**NSB day (RM)**
804	475	1,414	783
Sea-breeze probabilities (2000–2005)			
Identical SB days	**Identical NSB days**	**Different SB days**	**Different NSB days**
0.48	0.47	0.11	0.89

2.5 Trend analysis and statistics

Long-term trends for SB speeds, gusts and occurrence were estimated for 1961–2019. As a first step, we create daily time series of wind speed and wind gust for SB days in each weather station. From daily time series, we derive monthly averaged and monthly occurrence series. Weighted averages were performed by grouping all the SB days found in one same region to create regional and coastal series (see Table 2). After this step, we calculated the anomalies with respect to 1981–2010 to assure that no weather station dominated the averaged series (Zhang et al. 2020). Then, we estimated trends with a weighted linear regression in meters per second per decade ($m\ s^{-1}\ decade^{-1}$). Trend significance was assessed by applying the non-parametric modified Mann-Kendall test (Hamed and Rao 1998), which corrects the variance for highly autocorrelated series. Statistical significance was also assessed from a "process and importance" perspective, following McVicar et al. 2010 and Minola et al. 2021. This perspective uses three p-level thresholds, defined as (i) highly significant ($p < 0.05$); (ii) significant ($p < 0.10$) and (iii) not significant ($p > 0.10$). To evaluate the trend persistence, we performed running trends (Brunetti et al., 2006), which detect weakened or stronger trends sub-periods (Morán-Tejeda et al. 2016) with a minimum window length of 30 years, which runs from 1961 to 2019. We also computed a 15-year Gaussian low pass filter to illustrate the multidecadal variability of SB, and the coefficient of determination value (R^2) to estimate the variance between SB speeds and gusts. Lastly, calculations are performed over three different time scales: annually, monthly and boreal seasons: December, January and February (DJF) for winter; March, April and May (MAM) for spring; June, July and August (JJA) for summer; and September, October and November (SON) for autumn.

2.6 Atmospheric circulation indices

We selected four atmospheric circulation indices to assess their relationship (via Pearson's correlation coefficient (r) with the observed SB variability over the 58-year study: *(i)* The daily WeMOI (Martin-Vide

and Lopez-Bustins 2006) provided by the Group of Climatology at the University of Barcelona (http://www.ub.edu/gc/wemo/, last accessed February 24, 2022). This index is based on the regional sea-level pressure difference between the barometric dipole San Fernando (Cádiz) and Padua (Italy), a representation is shown in Fig. 1. We used it to detect potential SB passages for the Eastern Spain (Azorin-Molina and Lopez-Bustins 2008); *(ii)* The MOI (Palutikof 2003) provided by the Climate Research Unit (CRU), available online at https://crudata.uea.ac.uk/cru/data/moi/ (last accessed February 24, 2022); *(iii)* The NAOI (Jones et al. 1997) retrieved from CRU (https://crudata.uea.ac.uk/cru/data/nao/, last accessed February 24, 2022); and *(iv)* the SNAOI (Folland et al. 2009) calculated by averaging the NAOI values for July-August. These indices are well known to drive most of the climatic variability in the Eastern Spain (Corell et al. 2020; Martinez-Artigas et al. 2021), and some authors have analyzed their influence on wind speed variability for this region (Azorin-Molina et al. 2014a, 2016).

2.7 Local-scale drivers of SB activity

To estimate the possible relationship between SB trends, variability and local-physical factors, we computed the Pearson's correlation between the land-sea temperature difference and horizontal pressure gradient (PG) and our SB parameters (i.e., speeds, gusts and occurrence). To calculate the land-sea thermal contrast we obtained 2m air temperature data over land and ocean surfaces at 1200 UTC from ERA5 Reanalysis from 1979 onwards (https://cds.climate.copernicus.eu/cdsapp#!/dataset/reanalysis-era5-single-levels?tab=overview; last accessed February 24, 2022) and its preliminary back extension dataset reaching back 1950 (https://cds.climate.copernicus.eu/cdsapp#!/dataset/reanalysis-era5-single-levels-preliminary-back-extension?tab=overview; last accessed February 24, 2022), to cover the 1961–2019 period. The grid points defined to estimate the temperature differences are given in Table S3. Further to compute the horizontal PG, we obtained the ERA5's surface pressure from the Copernicus Climate Data Store, which is expressed as:

$$\mathrm{PG} = \left(\frac{\mathrm{SP}_{land} - \mathrm{SP}_{sea}}{\mathrm{D}} \right) * 100$$

where SP refers to surface pressure (in hPa) over land and sea surfaces, and D is the distance (in km) between grid points (described in Table S3).

3 Results

3.1 SB Climatology

Figure 3 displays the regional climatology of the SB occurrence across Eastern Spain for 1961–2019. In general, a marked seasonality of the SB is observed, with a greater occurrence in summer (up to 27 days per month), and a transition period in May and September. Further, the low (but not absent) occurrence of the SB in winter seems to increase slightly in recent years, although it does not exceed 21 days per month in any year. The 58-years climatology of the SB speeds and gusts is also presented in Fig. 4. The annual

climatology is dominated by the spring-summer season, therefore presenting a similar pattern. North-eastern and southern regions exhibited the largest values at all scales, while the smallest ones occurred in the eastern region. At the intra-annual scale, summer exhibited the highest SB speeds and gusts values (5.3 and 10.8 m s^{-1}, respectively), while strong differences were found among the regions in winter. The spatial climatology (1961–2019) of the mean, standard deviation, minimum and maximum SB speeds, gusts and occurrence (Fig. S2, S3 and S4, respectively) for 16 stations across the Eastern Spain are also presented in the supplemental material. It is remarkable the greater values in airport stations (i.e., rural areas) than in the cities in e.g., Alicante, Valencia and Mallorca locations, due to the effect of urbanization for all statistical parameters.

(Fig. 4 about here)

3.2 Trends in the SB speeds, gusts and occurrence

We found widespread opposite trends between SB speeds and gusts, shown in Tables 4a and 4b, as well as in Fig. 5. For 1961–2019, the regional SB speeds show significant decreases at all timescales, with an annual reduction of -0.07 m s^{-1} $decade^{-1}$ ($p < 0.05$). On the contrary, SB gusts presented non-significant increasing annual trends (+ 0.01 m s^{-1} $decade^{-1}$, $p > 0.10$). Seasonal trends of gusts are positive in winter (non-significant) and autumn (significant), and opposite negative slopes appear in spring and summer ($p > 0.10$). The weakening of the SB speeds and the strengthening of the SB gusts occurred during most of the 1961–2019 period (Fig. 5). It is noticeable the recent significant slowdown for the SB speeds in autumn-winter after a long period of non-significant stability or weak increases (Fig. 5b and 5c). Likewise, in recent years there has been a recent weakening of the winter SB gusts (Fig. 5b), while on the contrary, spring-summer ones began to reinforce.

Table 4

Annual and seasonal trends (m s^{-1} dec^{-1}) in the mean SB speeds (a), gusts (b), and occurrence (c) in all Eastern Spain and each coastal region for 1961–2019, abbreviated as southern (S), south-eastern (SE), eastern (E), north-eastern (NE), and Balearic Islands (BI). Statistically significant trends were defined as $p < 0.05$ (in italic bold and in parenthesis), and $p < 0.10$ (in italic bold).

		All	S	SE	E	NE	BI
(a)	**Annual**	(-0.074)	(-0.078)	(-0.100)	(-0.026)	(-0.043)	(-0.111)
	Winter (DJF)	-0.022	-0.043	(-0.067)	(+ 0.056)	(+ 0.055)	(-0.093)
	Spring (MAM)	(-0.109)	(-0.083)	(-0.133)	(-0.064)	(-0.146)	(-0.150)
	Summer (JJA)	(-0.106)	(-0.115)	(-0.102)	(-0.093)	(-0.134)	(-0.091)
	Autumn (SON)	(-0.054)	(-0.086)	(-0.100)	+ 0.016	+ 0.056	(-0.105)
(b)	**Annual**	+ 0.014	+ 0.031	-0.018	+ 0.067	+ 0.076	(-0.084)
	Winter (DJF)	+ 0.033	(+ 0.163)	-0.039	+ 0.111	+ 0.104	(-0.179)
	Spring (MAM)	-0.031	-0.004	-0.053	-0.038	-0.025	(-0.092)
	Summer (JJA)	-0.006	-0.008	-0.028	+ 0.036	-0.005	-0.034
	Autumn (SON)	(+ 0.064)	-0.008	+ 0.038	(+ 0.164)	(+ 0.227)	-0.008
(c)	**Annual**	+ 0.893	(+ 3.147)	+ 0.850	(+ 2.182)	+ 0.086	+ 0.710
	Winter (DJF)	(+ 1.724)	(+ 2.032)	(+ 1.404)	(+ 1.776)	(+ 0.638)	(+ 1.279)
	Spring (MAM)	-0.813	-0.166	-0.477	-0.646	-0.811	-0.275
	Summer (JJA)	(-0.578)	+ 0.352	-0.352	+ 0.091	-0.316	-0.198
	Autumn (SON)	+ 0.557	+ 0.615	+ 0.262	+ 0.525	+ 0.065	-0.385

(Fig. 5 about here)

In addition, we found contrasting spatial patterns on trends which influence the regional tendency. A marked slowdown in SB speeds was found all year round for coastal regions ($p < 0.05$; Table 4a), where the weakening significantly dominated 93.7% of the 16-station annual trends ($p < 0.05$; Fig. 6). Nevertheless, eastern and north-eastern regions (i.e., around 25% of the stations) displayed significant increases in autumn-winter ($p < 0.10$), although these began to weaken significantly in the recent years ($p < 0.10$; Fig. S4). SB gusts trends were overall heterogeneous and non-significant ($p > 0.10$, Fig. 6), but small increases dominated eastern and north-eastern regions in winter and autumn ($p < 0.05$; Fig. 6) while contrary, the decline was evident in spring for much of the stations, and persistent in the Balearic Islands for almost all seasons ($p < 0.05$; Fig. 6, Table 4b). Particularly, large cities (e.g., Barcelona and Valencia) evidenced opposing trends between airports and urban stations at annual and winter scale for both parameters.

The regional SB occurrence showed non-significant positive trends annually (+ 0.86 days decade^{-1}, $p >$ 0.10; Table 4c), highlighting the significant upward winter trend (+ 1.72 days decade^{-1}, $p < 0.05$) and the downward one in summer (-0.58 days decade^{-1}, $p < 0.01$). The increasing SB occurrence is even more evident at coastal level for the southern and eastern region with annual magnitudes of change of + 3.15 and + 2.18 days decade^{-1} respectively ($p < 0.05$, Table 4c), with a remarkable significant positive trend in winter for all regions ($p < 0.05$, Table 4c). Lastly, it is worth noting the upward trends at airport stations compared to the decline in urban stations within the same city (e.g., Alicante or Valencia). This is a clear feature of the effect of the local surface roughness.

(Fig. 6 about here)

3.3 Multidecadal variability of the SB speeds, gusts and days

The regional annual and seasonal multidecadal variability of SB speeds, gusts and occurrence for 1961–2019 are shown in Fig. 7. Overall, the 15-year Gaussian low-pass filter revealed a decoupled variability between SB speeds and gusts that in terms of r and R^2. This clearly occurs at the annual scale, as well as in summer. For these time-scales, anomalies for SB speeds decreased and for SB gusts increased with simultaneous changes for both parameters around the 1990s. The strongest intra-annual variability of anomalies occurred in winter (Fig. 7b), especially for SB gusts, with the weakest one in summer (Fig. 7d). Winter also presents a strong positive correlation between SB speeds and gusts variability (r = 0.68 and R^2 = 0.46; Fig. 7), the same for spring and autumn. For the SB occurrence, it is remarkable the increasing variability observed in winter (+ 1.72 days decade^{-1}, $p < 0.05$) and the decreasing trend in summer (-0.58 days decade^{-1}, $p < 0.05$). It is evident from Fig. 8 that coastal series also showed a decoupled pattern, especially in the north-eastern region.

(Fig. 7 about here)

(Fig. 8 about here)

3.4 Influence of large-scale circulation and physical-local drivers

Figure 9,10,11 show spatial r correlations between SB time series and large-scale circulation indices. These statistical relationships are better captured when stations are grouped into coastal regions (Tables 5–7). Overall, we found that the WeMOI exerted its major influence on SB speeds at the annual scale and in spring for all regions ($p < 0.05$; Table 5, Fig. 10). The positive correlation is stronger in the south-eastern in all time-scales ($p < 0.10$), except for winter, when reverses its sign. Particularly, this positive relationship between SB speeds and the WeMOI may be related to its tendency towards negative phases at all time scales ($p < 0.05$ excepting winter; Table 5). Other atmospheric indices, such as the MOI and the SNAOI partly influenced SB speeds in summer for specific regions or stations. Moreover, the results for the SB gusts were not conclusive, with very few significant correlations, most of them heterogeneous and weak

in specific regions at different time scales (Table 6). For the SB occurrence, there is a significant positive relationship with the NAOI at all timescales ($p < 0.05$; Table 7; Fig. 9), followed by the MOI that also exerted a strong positive and significant influence on the SB days both annually and seasonally, except in summer ($p < 0.05$; Table 7; Fig. 11), while the WeMOI only showed a negative and significant correlation in winter, but positive in autumn for all coastal regions.

(Fig. 9 about here)

(Fig. 10 about here)

(Fig. 11 about here)

Table 5

Trends (dec^{-1}) of annual and seasonal WeMOI, MOI, NAOI, and SNAOI for 1961–2019 and their Pearson's correlation coefficients (*r*) with the SB speeds in all Eastern Spain and each coastal region, abbreviated as southern (S), south-eastern (SE), eastern (E), north-eastern (NE), and Balearic Islands (BI). Statistically significant trends and correlations were defined as $p < 0.05$ (in italic bold and in parenthesis), and $p < 0.10$ (in italic bold).

			r					
		Trend	**All**	S	**SE**	**E**	**NE**	BI
WeMOI	**Annual**	(-0.16)	(+ 0.38)	+ 0.20	(+ 0.56)	+ 0.23	+ 0.11	(+ 0.31)
	Winter (DJF)	-0.04	-0.12	-0.24	-0.22	+ 0.03	-0.17	+ 0.01
	Spring (MAM)	(-0.27)	(+ 0.46)	+ 0.24	(+ 0.48)	(+ 0.37)	(+ 0.29)	(+ 0.42)
	Summer (JJA)	(-0.17)	+ 0.25	+ 0.09	(+ 0.39)	+ 0.15	+ 0.12	+ 0.17
	Autumn (SON)	(-0.17)	+ 0.13	+ 0.11	(+ 0.35)	-0.06	-0.03	+ 0.03
MOI	**Annual**	-0.01	+ 0.14	-0.16	+ 0.07	(+ 0.26)	+ 0.12	+ 0.16
	Winter (DJF)	(+ 0.04)	-0.08	-0.09	-0.12	+ 0.03	+ 0.08	+ 0.10
	Spring (MAM)	(-0.03)	+ 0.12	-0.02	+ 0.18	-0.00	+ 0.19	+ 0.17
	Summer (JJA)	(-0.02)	(+ 0.29)	+ 0.09	+ 0.25	+ 0.20	+ 0.22	(+ 0.27)
	Autumn (SON)	-0.02	+ 0.18	+ 0.15	+ 0.12	-0.09	+ 0.15	+ 0.16
NAOI	**Annual**	-0.01	+ 0.11	-0.13	+ 0.05	+ 0.18	+ 0.09	+ 0.10
	Winter (DJF)	+ 0.19	-0.08	-0.07	-0.11	-0.04	+ 0.10	+ 0.04
	Spring (MAM)	+ 0.05	-0.12	-0.06	-0.11	-0.19	+ 0.06	-0.03
	Summer (JJA)	-0.15	+ 0.10	+ 0.09	+ 0.06	+ 0.09	+ 0.06	+ 0.04
	Autumn (SON)	(-0.14)	+ 0.09	+ 0.07	+ 0.00	-0.03	-0.09	+ 0.14
SNAOI	Summer (JA)	-0.13	(+ 0.32)	(+ 0.30)	+ 0.11	+ 0.12	+ 0.15	+ 0.15

Table 6
As Table 5 but for the SB gusts.

		r						
		Trend	**All**	S	**SE**	**E**	**NE**	BI
WeMOI	**Annual**	(-0.16)	-0.18	-0.00	+ 0.09	(-0.31)	(-0.28)	+ 0.15
	Winter (DJF)	-0.04	+ 0.00	-0.14	+ 0.01	+ 0.05	-0.18	+ 0.05
	Spring (MAM)	(-0.27)	+ 0.24	+ 0.17	+ 0.07	+ 0.25	+ 0.10	(+ 0.27)
	Summer (JJA)	(-0.17)	-0.18	+ 0.08	+ 0.06	(-0.28)	-0.16	-0.10
	Autumn (SON)	(-0.17)	-0.01	+ 0.14	+ 0.12	-0.09	-0.15	+ 0.02
MOI	**Annual**	-0.01	+ 0.20	+ 0.19	+ 0.05	+ 0.13	+ 0.09	+ 0.11
	Winter (DJF)	(+ 0.04)	-0.09	+ 0.09	(-0.32)	+ 0.06	-0.02	-0.12
	Spring (MAM)	(-0.03)	-0.03	+ 0.08	-0.05	-0.10	+ 0.14	+ 0.13
	Summer (JJA)	(-0.02)	(+ 0.36)	+ 0.15	+ 0.13	+ 0.12	(+ 0.30)	(+ 0.28)
	Autumn (SON)	-0.02	-0.06	+ 0.04	-0.12	+ 0.00	+ 0.01	+ 0.02
NAOI	**Annual**	-0.01	+ 0.17	+ 0.08	-0.01	+ 0.13	+ 0.02	+ 0.03
	Winter (DJF)	+ 0.19	-0.13	-0.01	(-0.31)	-0.01	-0.01	-0.21
	Spring (MAM)	+ 0.05	+ 0.00	+ 0.04	-0.14	-0.18	+ 0.23	+ 0.16
	Summer (JJA)	-0.15	-0.12	-0.12	-0.12	-0.09	-0.05	-0.01
	Autumn (SON)	(-0.14)	-0.14	+ 0.06	(-0.32)	-0.01	-0.20	-0.01
SNAOI	Summer (JA)	-0.13	+ 0.07	-0.03	-0.08	-0.08	-0.19	-0.07

Table 7
As Table 5 but for the SB days.

		r						
		Trend	**All**	S	**SE**	**E**	**NE**	**BI**
WeMOI	**Annual**	(-0.16)	+ 0.08	-0.09	+ 0.16	+ 0.01	+ 0.16	+ 0.18
	Winter (DJF)	-0.04	(-0.31)	(-0.27)	(-0.28)	(-0.28)	(-0.27)	-0.21
	Spring (MAM)	(-0.27)	-0.09	-0.03	+ 0.01	+ 0.05	+ 0.09	+ 0.08
	Summer (JJA)	(-0.17)	-0.11	-0.03	+ 0.06	+ 0.00	+ 0.04	+ 0.09
	Autumn (SON)	(-0.17)	(-0.32)	(+ 0.38)	(+ 0.34)	(+ 0.34)	(+ 0.29)	(+ 0.40)
MOI	**Annual**	-0.01	(+ 0.27)	(+ 0.31)	(+ 0.31)	(+ 0.31)	(+ 0.33)	+ 0.22
	Winter (DJF)	(+ 0.04)	(+ 0.43)	(+ 0.52)	(+ 0.48)	(+ 0.53)	(+ 0.41)	(+ 0.48)
	Spring (MAM)	(-0.03)	(+ 0.31)	(+ 0.26)	+ 0.20	(+ 0.31)	(+ 0.40)	(+ 0.32)
	Summer (JJA)	(-0.02)	-0.04	-0.09	-0.06	-0.07	+ 0.13	-0.07
	Autumn (SON)	-0.02	(+ 0.57)	(+ 0.62)	(+ 0.51)	(+ 0.59)	(+ 0.46)	(+ 0.48)
NAOI	**Annual**	-0.01	+ 0.25	(+ 0.29)	(+ 0.26)	(+ 0.29)	(+ 0.26)	+ 0.25
	Winter (DJF)	+ 0.19	(+ 0.42)	(+ 0.55)	(+ 0.46)	(+ 0.54)	(+ 0.40)	(+ 0.53)
	Spring (MAM)	+ 0.05	(+ 0.46)	(+ 0.47)	(+ 0.36)	(+ 0.47)	(+ 0.51)	(+ 0.43)
	Summer (JJA)	-0.15	(+ 0.03)	+ 0.23	(+ 0.31)	(+ 0.31)	(+ 0.32)	+ 0.24
	Autumn (SON)	(-0.14)	(+ 0.45)	(+ 0.48)	(+ 0.45)	(+ 0.49)	(+ 0.43)	(+ 0.49)
SNAOI	Summer (JA)	-0.13	-0.08	+ 0.07	+ 0.05	+ 0.05	-0.03	-0.09

For the 26 JC weather types, the highest positive correlations occurred for the SB days (Fig. 12c), where the A regime enhanced the occurrence of SB events regionally from autumn till spring (+ 0.6 > r < + 0.8, p < 0.05), followed by the E, NE and AE types (p < 0.05), which exerted a strong influence throughout the year, especially in summer. It is worth mentioning that at coastal level, the summer SB occurrence is clearly

inhibited by westerlies, although a frequent anomalous easterly advection may enhance it ($p < 0.10$; Fig. S13). The most remarkable results for the SB speeds (Fig. 12a) and gusts (Fig. 12b) were their significant negative relationship with the A regime ($p < 0.05$; except in summer), denoting that a stable atmosphere weakens SB circulations. Other weather types (i.e., E, N, NE and NW) partly exerted some positive and significant relationships with both parameters, but these results should be carefully examined at the local level (Fig. S10).

(Fig. 12 about here)

Finally, the influence of the local-physical drivers on the SB is complex. First, the SB speeds showed a strong and widespread negative relationship with land-sea temperature difference at annual scale and in spring and summer (Fig. 13); i.e., unexpectedly, the greater the contrast is, the weaker SB speed blow. Surprisingly, the SB speeds do not present a strong relationship with the local pressure gradient (Table 8). Second, most correlations of both the land-sea temperature difference and local pressure gradient with the SB gusts are weak or non-significant and do not follow a pattern, which suggest that gusts are driven by other local mechanisms in comparison to the SB speeds. Third and last, land-sea temperature difference is positively but not significantly correlated with the SB occurrence; whereas the pressure gradient barely shows an influence on this.

(Fig. 13 about here)

Table 8

Annual and seasonal Pearson's correlations of land-sea temperature difference and local pressure gradient with the SB speeds (a), SB gusts (b) and SB occurrence (c) for each coastal region of Eastern Spain, abbreviated as southern (S), south-eastern (SE), eastern (E), north-eastern (NE), and Balearic Islands (BI). Statistically significant correlations were defined as $p < 0.05$ (in italic bold and in parenthesis), and $p < 0.10$ (in italic bold).

			S	SE	E	NE	BI
(a)	**Land-sea temperature difference (1961–2019)**	**Annual**	(-0.45)	(-0.56)	(-0.31)	-0.24	(-0.39)
		Winter (DJF)	(-0.43)	(-0.46)	-0.04	+ 0.05	(-0.33)
		Spring (MAM)	(-0.38)	(-0.30)	(-0.25)	(-0.35)	(-0.28)
		Summer (JJA)	(-0.41)	(-0.31)	(-0.29)	(-0.39)	(-0.30)
		Autumn (SON)	(-0.32)	(-0.46)	+ 0.14	+ 0.17	(-0.28)
	Local pressure gradient (1961–2019)	**Annual**	-0.22	+ 0.22	-0.04	+ 0.02	-0.19
		Winter (DJF)	+ 0.02	+ 0.16	-0.07	+ 0.20	(+ 0.17)
		Spring (MAM)	-0.03	(+ 0.33)	(-0.30)	+ 0.18	+ 0.02
		Summer (JJA)	-0.17	+ 0.04	(-0.40)	(-0.32)	-0.22
		Autumn (SON)	-0.25	-0.03	-0.07	+ 0.06	+ 0.18
(b)							
	Land-sea temperature difference (1961–2019)	**Annual**	+ 0.08	-0.18	+ 0.23	+ 0.21	(-0.29)
		Winter (DJF)	-0.06	(-0.33)	-0.02	+ 0.11	(-0.43)
		Spring (MAM)	-0.00	-0.11	+ 0.12	+ 0.12	-0.02
		Summer (JJA)	-0.02	-0.05	+ 0.25	+ 0.15	-0.02
		Autumn (SON)	+ 0.04	-0.20	(+ 0.47)	(+ 0.29)	-0.14
	Local pressure gradient (1961–2019)	**Annual**	+ 0.24	-0.03	+ 0.05	-0.11	-0.16
		Winter (DJF)	+ 0.14	-0.25	(-0.31)	(+ 0.37)	+ 0.05
		Spring (MAM)	(+ 0.26)	+ 0.06	-0.10	-0.20	-0.15
		Summer (JJA)	(+ 0.26)	+ 0.04	+ 0.05	(-0.30)	(-0.33)
		Autumn (SON)	+ 0.21	-0.22	-0.21	(+ 0.29)	+ 0.05

			S	SE	E	NE	BI
(c)	**Land-sea temperature difference (1961–2019)**	**Annual**	(+ 0.30)	+ 0.21	+ 0.25	+ 0.08	+ 0.06
		Winter (DJF)	+ 0.18	+ 0.17	+ 0.21	(+ 0.40)	(+ 0.35)
		Spring (MAM)	+ 0.15	+ 0.24	+ 0.20	+ 0.17	+ 0.22
		Summer (JJA)	-0.12	-0.08	+ 0.12	+ 0.04	-0.15
		Autumn (SON)	+ 0.24	+ 0.24	(+ 0.36)	+ 0.18	+ 0.14
	Local pressure gradient (1961–2019)	**Annual**	+ 0.04	+ 0.12	+ 0.03	-0.09	-0.05
		Winter (DJF)	-0.10	+ 0.05	-0.13	+ 0.08	+ 0.02
		Spring (MAM)	(+ 0.31)	(+ 0.24)	+ 0.09	(-0.32)	-0.11
		Summer (JJA)	+ 0.28	+ 0.06	-0.02	-0.24	+ 0.20
		Autumn (SON)	-0.07	-0.00	-0.14	-0.10	-0.15

4 Discussion

This study investigated for the first time long-term changes in the SB speeds, gusts and occurrence across Eastern Spain for 1961–2019. We proposed a novel automated method to identify past SB events by applying six alternative test criteria, with the goal to create the longest (58-years) available database of potential SB episodes across the Spanish Mediterranean coast, and to provide new knowledge about the multidecadal climate and variability of this local wind. Our method represents an alternative technique to identify potential events of SB in areas in which long-climate records over land and sea surfaces are limited. By using a minimum number of variables (Laird et al. 2001), it can be easily applied worldwide in regions with a regional sea-level pressure difference (Azorin-Molina and Lopez-Bustins, 2008).

Our main findings reveal new evidence regarding the changes in SB in the Eastern Spain, a region in which SB represent the most frequent local wind circulation throughout the year (Olcina-Cantos and Azorin-Molina 2004; Azorin-Molina and Martín-Vide 2007). Our results also represent new insights into the *stilling* vs. *reversal* phenomena (Roderick et al. 2007; Zeng et al. 2019; Zhang et al. 2020), as it is focused on improving our understanding of seasonal changes of the near-surface wind speeds and gusts driven by local winds. Here we showed a decoupled variability and trends between SB speeds and gusts, which represents a finding never reported before for local winds. Actually, our results also showed that the understanding of SB changes is challenging, as many local factors can occur at the same time and

drivers differ between mean and gust speeds (Miller et al. 2003; Shen et al. 2019, 2021b). A specific discussion of the principal findings of this research follows:

4.1 Increased SB occurrence due to anticyclonic activity and other related large-scale dynamics

The overall increase in the annual SB occurrence is in agreement with some global analyses (Jiang et al. 2010; Perez et al. 2017; Shen and Zhao 2020), but this trend may not be a widespread phenomenon (Pazandeh-Masouleh et al. 2019; Shen et al. 2019). Specifically, the tendency of SB in Eastern Spain suggests that it is becoming a less common phenomenon in summer, one result similar to that found in Shangai (Shen et al. 2019) but in discordance with the hypothetical increase induced by the air-temperature rise (Lebassi-Habtezion et al. 2011; Perez et al. 2017). In contrast, the increased winter SB days have never been reported in long climatological studies, as most research have focused on summer SB. Based on our correlations with large-scale circulation, we hypothesize that more frequent anticyclonic conditions (i.e., calm and dry days) strengthen the SB occurrence during cold months (Giorgi and Lionello 2008; Zhang et al. 2012; Rojas et al. 2013; Otero et al. 2018; Seager et al. 2019). The increase of the SB occurrence is also strongly related to the E and NE types, while other regimes such as the AE, ANE, N, and SE partly favor it, agreeing with previous studies (Azorin-Molina et al. 2011a); although with few differences depending on the region (Fig. S10-S14). The most evident pattern found seasonally is the negative effect of westerlies and NW on inhibiting the summer occurrence (Fig. S13), although anomalous easterly advection enhance it (Haarsma et al. 2009; Zhang et al. 2012; Fernández-González et al. 2012).

In addition, it is worth to mention that winter anticyclonic circulations over the region (and therefore SB activity) may be favored by the NAOI+ (Fernández-González et al. 2012). The strong correlation found between NAOI and SB days provide plausible insights about the dominant relationship between NAOI+, A regime and the increased SB activity over the region in winter, despite this teleconnection index is thought to not represent well the atmospheric variability of the eastern Iberian Peninsula (Martin-Vide and Lopez-Bustins 2006). However, the non-significant trend of NAOI towards positive phases in winter versus the significant negative one in summer-autumn difficult the understanding of its positive correlation with the SB occurrence in all time scales. Other atmospheric oscillations such as MOI also contribute positively the SB activity, but it is negatively correlated in summer. Given that NAO and MO have shown to be strongly linked in winter (Angulo-Martínez and Beguería, 2012), it is possible that coupled modes of atmospheric circulation or their interaction with local mechanisms that take place in the warm months could have a greater weight in explaining the occurrence of the summer SB.

4.2 Uncertainties in the mechanisms driving decoupled SB speeds and gusts

Different studies indicate that global warming is enhancing stability in mid-latitudes due to subsidence that may cause more frequent but weaker SB circulations (Giorgio and Limonello 2008; Zappa et al. 2015;

Deng et al. 2021). This is consistent with our findings of higher SB activity but weakened SB speeds throughout the year. Our results suggest that anticyclonic situations may be behind the decline of the SB speeds, but the land-sea temperature difference seems to also play a significant role on the declining trends in most stations and seasons. This sheds light over recent works suggest that the weakening of summer local winds in Western Europe is due to the effect of air-temperature rise and ocean warming (e.g., the Atlantic warm pool or the Mediterranean hot spot) on reducing the land-sea thermal gradient (Misra et al. 2011; Tuel and Eltahir 2020; Real et al. 2021). Other authors suggested the effect of urban expansion and irrigation patterns on SB speeds declining (Jiang et al. 2010; Vahmani et al. 2016; Shen et al. 2019; Shen and Zhao 2020), being mechanisms that may further explain local-based trends (especially in autumn-winter), as well as the opposing ones between rural and urban stations. Finally, the decline in the SB speeds is contrary to the generalized hypothesis about a reinforced SB driving intensified coastal summer winds (Lebassi-Habtezion et al. 2011; Vahmani and Ban-Weiss 2016; Azorin-Molina et al. 2018a; Zhang et al. 2020), and specifically converse with the increasing summer near-surface wind speeds trend reported for Spain (Azorin-Molina et al. 2014a, 2016).

The opposite positive trends of the SB gusts introduce complexity to the explanation of the variability of local-winds. These were spatially heterogeneous in sign and magnitude, suggesting the influence of local-based drivers. However, our findings are not conclusive in regards the mechanisms behind the SB gusts despite having analyzed their relationship with large-scale circulation, land-sea gradient and even some preliminary test with the Normal Difference Vegetation Index (NDVI) indices (see supplemental material). Parameters such as (i) land degradation and topography (Miao et al. 2003; Marshall et al. 2004); (ii) air temperature warming (Pazandeh-Masouleh et al. 2019); (iii) soil depletion (Diffenbaugh et al. 2005; Grau et al. 2021); (iv) and onshore synoptic flows and their interaction with orography (Zecchetto and De Biasio 2007; Azorin-Molina and Chen 2009) have been suggested to strongly influence wind extremes (e.g., SB gusts and fronts). It is widely addressed that climate change is enhancing extreme events (Chen et al. 2020), being these driven by local-scale features and processes amplifying their responses and causing stronger gusts (Diffenbaugh et al. 2005; Tuel and Eltahir 2020; Azorin-Molina et al. 2021). For SB, the influence of large-scale synoptic winds (e.g., offshore flows produce higher SB gusts; Azorin-Molina and Chen, 2009) could be also behind the decoupled tendency between the SB speeds and gusts. Future attribution research is needed for unrevealing the causes behind this phenomenon.

4.3 Overview, possible implications and final remarks

To summarize, although some few works have reported opposite trends in SB, e.g., the decreasing summer SB speed in China (Jiang et al. 2010; Shen et al. 2019) or the strengthening of SB gusts in Australia (Pazandeh-Masouleh et al. 2019), opposite trends in regional SB speeds and gusts have never been reported in the literature for Eastern Spain. It is worth mentioning that the strengthening of the SB gusts corresponds with the increase of the near-surface wind gusts in the Iberian Peninsula during the warm months for specific stations (Azorin-Molina et al. 2016). However, the comparison with other results is not straightforward due to the differences in spatial and temporal scales, being the trend analysis of wind speeds sensitive to the period and region taken into account (McVicar et al. 2010; Troccoli et al.

2012). Furthermore, the local-based nature of SB makes the trend comparison between regions even more complex, and SB research have no reported a pattern on global variability and trends of this local wind (Shen et al. 2021b). Likewise, the drivers of these changes may be different (Shen et al. 2019; Pazandeh-Masouleh et al. 2019; Shen et al. 2021b). Among the various mechanisms investigated here, we did not find the processes behind the increasing SB gusts and its decoupling variability with the SB speeds, an uncertainty that still need to be fully understood. With this in mind, one robust approach to better attribute this phenomenon would be to develop sensitivity studies with regional-local climate models; i.e., by integrating all natural and anthropogenic forcing such as fine-scale land-sea difference, horizontal pressure gradient, land-use changes, soil drying, large-scale synoptic flows, orography, urbanization, among many others (Zhang et al. 2021).

Our results are based on the largest available dataset of observed near-surface wind speed data in Eastern Spain, even though a longer period or a larger number of stations might help to confirm our findings or to answer some remaining questions. We used low-temporal resolution data (i.e., 3 subdaily observations) to calculate daily means of SB speed, one approach that may not capture the whole picture of SB changes but detects regional trends and, at the same time, distinguishes local peculiarities. In addition, the limited spatial resolution of observed weather data over ocean and land made difficult to analyze trends of SB characteristics (e.g., inland penetration, onset, duration, etc.) but also physical mechanisms controlling it. The use of re-analysis data to calculate the land-sea temperature difference and horizontal pressure gradient, daily precipitation, or wind direction could leave a considerable margin of error, especially in trying to explain the potential causes as they not represent well fine-scale features and processes (Diffenbaugh et al. 2005; Millán 2014; Tierney et al. 2017; Tetzner et al. 2019).

We end by emphasizing the increasing frequency of anticyclonic circulation, inducing persistent SB activity but weaker speeds. This has been previously suggested in previous works, with indications that it could favor the wind industry (Jiang et al. 2010). It is also very interesting that a decrease in the SB speeds does not exclude a winter increase in its extremes, e.g., SB gusts and fronts (Laurila et al. 2021), possibly due to the direct or collateral effect of global warming on changes in atmospheric circulation and land uses (Miao et al. 2003). However, the weakening of summer SB speeds, and the declining of its activity may be explain reductions in summer inland precipitation with implications in amplifying droughts, land aridity and exacerbating wildfires (Millán et al. 2005; Pastor et al. 2015; Pausas and Millán 2019). In specific locations stronger but drier gusts may occur as response of the combined effect of air-temperature rise and soil depletion, urbanization and land degradation on reducing the moisture available for SB (Pausas and Millán 2019; Guion et al. 2021). The foregoing shows the implications of filling a research niche of changes in SB on various socioeconomic and environmental spheres.

5 Conclusions

The main findings of the long-term trends and variability of sea breeze occurrence, speeds and gusts in Eastern Spain for 1961–2019 are:

1. The SB occurrence increased annually (+ 0.89 days per decade, $p > 0.10$) and in winter (+ 1.72 days per decade, $p < 0.05$). On the contrary, summer SB days decreased at a rate of -0.58 days decade^{-1} ($p < 0.05$).

2. Opposite trends were observed between the SB speeds (-0.07 m s^{-1} dec^{-1}, $p < 0.05$) and the SB gusts (+ 0.01 m s^{-1} dec^{-1}, $p > 0.10$) with distinct seasonality, i.e., the SB speeds significantly decreased in spring-summer (-0.11 m s^{-1} dec^{-1}, $p < 0.05$), while the SB gusts increased ($p > 0.10$) in autumn-winter.
3. Trends in the winter SB occurrence are thought to be exerted by frequent anomalous anticyclonic conditions and the NAOI + and MOI+, while inhibiting the SB speeds and gusts. The declining of the SB speeds is mainly due to the influence of land-sea air temperature contrast and the A regime while the SB gusts reinforcement remain misunderstood. Future sensitivity studies using climate models could help to better understand the drivers controlling their variability in a warming climate.

Declarations

Funding

This research was funded by the following projects: IBER-STILLING (RTI2018-095749-A-I00); and VENTS (GVA-AICO/2021/023). C.A.M was granted by Ramon y Cajal fellowship (RYC-2017-22830).

Competing Interest

The authors have no relevant financial or non-financial interests to disclose.

Author Contributions

All authors contributed to the study conception and design. Material preparation, data collection and analysis were performed by S.B.V, C.A.M and J.G. The first draft of the manuscript was written by S.B.V and C.A.M, and all authors commented on previous versions of the manuscript. All authors read and approved the final manuscript.

Data Availability Statement.

Wind speeds and gusts data from weather stations were obtained from AEMET. Daily WeMO index was provided from the Climate Group of the University of Barcelona (http://www.ub.edu/gc/wemo/). Furthermore, NAO and MO indexes were retrieved from CRU (https://crudata.uea.ac.uk/cru/data/nao/; https://crudata.uea.ac.uk/cru/data/moi/). ERA5 Reanalysis and its back-extension were downloaded from Copernicus Climate Data Store (https://cds.climate.copernicus.eu/), while the NDVI was retrieved from the Laboratory of Climate Services and Climatology (https://spainndvi.csic.es/).The daily JC scheme weather types classification is available upon request to the corresponding author.

Acknowledgments.

We thank to AEMET for the observed wind speed data. This research was funded by the following projects: IBER-STILLING (RTI2018-095749-A-I00); and VENTS (GVA-AICO/2021/023). C.A.M was granted by Ramon y Cajal fellowship (RYC-2017-22830).

References

1. Alexandersson H (1986) A homogeneity test applied to precipitation data. J Climatol. https://doi.org/10.1002/joc.3370060607
2. Alomar G, Grimalt M (2008) Un modelo de simultaneidad de las brisas marinas en Mallorca. In: Sigró J, Brunet M, i Aguilar E (eds) Cambio climático regional y sus impactos. Publicaciones de la Asociación Española de Climatología (AEC). Ser. A.
3. Angulo-Martínez M, Beguería S (2012) Do atmospheric teleconnection patterns influence rainfall erosivity? A study of NAO, MO and WeMO in NE Spain, 1955–2006. J Hydrol. https://doi.org/10.1016/j.jhydrol.2012.04.063
4. Arrillaga JA, de Arellano JVG, Bosveld F et al (2018) Impacts of afternoon and evening sea-breeze fronts on local turbulence, and on CO2 and radon-222 transport. Q J R Meteorol Soc. https://doi.org/10.1002/qj.3252
5. Arrillaga JA, Jiménez P, Vilà-Guerau de Arellano J et al (2020) Analyzing the Synoptic-, Meso- and Local- Scale Involved in Sea Breeze Formation and Frontal Characteristics. J Geophys Res Atmos. https://doi.org/10.1029/2019JD031302
6. Azorin-Molina C, Martín-Vide J (2007) Methodological approach to the study of the daily persistence of the sea breeze in Alicante (Spain). Atmosfera
7. Azorin-Molina C, Lopez-Bustins JA (2008) An automated sea breeze selection technique based on regional sea-level pressure difference: WeMOi. Int J Climatol. https://doi.org/10.1002/joc.1663
8. Azorin-Molina C, Chen D (2009) A climatological study of the influence of synoptic-scale flows on sea breeze evolution in the Bay of Alicante (Spain). https://doi.org/10.1007/s00704-008-0028-2. Theor Appl Climatol
9. Azorin-Molina C, Connell BH, Baena-Calatrava R (2009) Sea-breeze convergence zones from AVHRR over the Iberian Mediterranean area and the Isle of Mallorca, Spain. J Appl Meteorol Climatol. https://doi.org/10.1175/2009JAMC2141.1
10. Azorin-Molina C, Chen D, Tijm S, Baldi M (2011a) A multi-year study of sea breezes in a Mediterranean coastal site: Alicante (Spain). Int J Climatol. https://doi.org/10.1002/joc.2064
11. Azorin-Molina C, Tijm S, Chen D (2011b) Development of selection algorithms and databases for sea breeze studies. Theor Appl Climatol. https://doi.org/10.1007/s00704-011-0454-4
12. Azorin-Molina C, Vicente-Serrano SM, Mcvicar TR et al (2014a) Homogenization and assessment of observed near-surface wind speed trends over Spain and Portugal, 1961–2011. J Clim. https://doi.org/10.1175/JCLI-D-13-00652.1

13. Azorin-Molina C, Tijm S, Ebert EE et al (2014b) Sea breeze thunderstorms in the eastern Iberian Peninsula. Neighborhood verification of HIRLAM and HARMONIE precipitation forecasts. Atmos Res. https://doi.org/10.1016/j.atmosres.2014.01.010
14. Azorin-Molina C, Tijm S, Ebert EE et al (2015) High Resolution HIRLAM Simulations of the Role of Low-Level Sea-Breeze Convergence in Initiating Deep Moist Convection in the Eastern Iberian Peninsula. https://doi.org/10.1007/s10546-014-9961-z. Boundary-Layer Meteorol
15. Azorin-Molina C, Guijarro JA, McVicar TR et al (2016) Trends of daily peak wind gusts in Spain and Portugal, 1961–2014. J Geophys Res. https://doi.org/10.1002/2015JD024485
16. Azorin-Molina C, Rehman S, Guijarro JA et al (2018a) Recent trends in wind speed across Saudi Arabia, 1978–2013: a break in the stilling. Int J Climatol. https://doi.org/10.1002/joc.5423
17. Azorin-Molina C, Menendez M, McVicar TR et al (2018b) Wind speed variability over the Canary Islands, 1948–2014: focusing on trend differences at the land–ocean interface and below–above the trade-wind inversion layer. Clim Dyn. https://doi.org/10.1007/s00382-017-3861-0
18. Azorin-Molina C, Guijarro JA, McVicar TR et al (2019) An approach to homogenize daily peak wind gusts: An application to the Australian series. Int J Climatol. https://doi.org/10.1002/joc.5949
19. Azorin-Molina C, McVicar TR, Guijarro JA et al (2021) A decline of observed daily peak wind gusts with distinct seasonality in Australia, 1941–2016. J Clim. https://doi.org/10.1175/JCLI-D-20-0590.1
20. Bei N, Zhao L, Wu J et al (2018) Impacts of sea-land and mountain-valley circulations on the air pollution in Beijing-Tianjin-Hebei (BTH): A case study. Environ Pollut. https://doi.org/10.1016/j.envpol.2017.11.066
21. Brunetti M, Maugeri M, Nanni T et al (2006) Precipitation variability and changes in the greater Alpine region over the 1800–2003 period. J Geophys Res Atmos. https://doi.org/10.1029/2005JD006674
22. Cana L, Grisolía-Santos D, Hernández-Guerra A (2020) A Numerical Study of a Sea Breeze at Fuerteventura Island, Canary Islands, Spain. https://doi.org/10.1007/s10546-020-00506-z. Boundary-Layer Meteorol
23. Chen D, Rodhe H, Emanuel K et al (2020) Summary of a workshop on extreme weather events in a warming world organized by the Royal Swedish Academy of Sciences. Tellus Ser B Chem Phys Meteorol. https://doi.org/10.1080/16000889.2020.1794236
24. Corell D, Estrela MJ, Valiente JA et al (2020) Influences of synoptic situation and teleconnections on fog-water collection in the Mediterranean Iberian Peninsula, 2003–2012. Int J Climatol. https://doi.org/10.1002/joc.6398
25. Coulibaly A, Omotosho BJ, Sylla MB et al (2019) Characteristics of land and sea breezes along the Guinea Coast of West Africa. Theor Appl Climatol. https://doi.org/10.1007/s00704-019-02882-0
26. Curci G, Guijarro JA, Di Antonio L et al (2021) Building a local climate reference dataset: Application to the Abruzzo region (Central Italy), 1930–2019. Int J Climatol. https://doi.org/10.1002/joc.7081
27. Davis SR, Farrar JT, Weller RA et al (2019) The Land-Sea Breeze of the Red Sea: Observations, Simulations, and Relationships to Regional Moisture Transport. J Geophys Res Atmos. https://doi.org/10.1029/2019JD031007

28. Deng K, Azorin-Molina C, Minola L et al (2021) Global near-surface wind speed changes over the last decades revealed by reanalyses and CMIP6 model simulations. J Clim. https://doi.org/10.1175/JCLI-D-20-0310.1
29. Diffenbaugh NS, Pal JS, Trapp RJ, Giorgi F (2005) Fine-scale processes regulate the response of extreme events to global climate change. Proc Natl Acad Sci U S A. https://doi.org/10.1073/pnas.0506042102
30. Drobinski P, Bastin S, Arsouze T et al (2018) North-western Mediterranean sea-breeze circulation in a regional climate system model. Clim Dyn. https://doi.org/10.1007/s00382-017-3595-z
31. El-Geziry TM, Elbessa M, Tonbol KM (2021) Climatology of Sea–Land Breezes Along the Southern Coast of the Levantine Basin. Pure Appl Geophys. https://doi.org/10.1007/s00024-021-02726-x
32. Fernández-González S, Del Río S, Castro A et al (2012) Connection between NAO, weather types and precipitation in León, Spain (1948–2008). Int J Climatol. https://doi.org/10.1002/joc.2431
33. Folland CK, Knight J, Linderholm HW et al (2009) The summer North Atlantic oscillation: Past, present, and future. J Clim. https://doi.org/10.1175/2008JCLI2459.1
34. Gavit P, Baddour Y, Tholmer R (2009) Use of change-point analysis for process monitoring and control. BioPharm Int
35. Giorgi F, Lionello P (2008) Climate change projections for the Mediterranean region. Glob Planet Change. https://doi.org/10.1016/j.gloplacha.2007.09.005
36. Grau A, Jiménez MA, Cuxart J (2021) Statistical characterization of the sea-breeze physical mechanisms through in-situ and satellite observations. Int J Climatol. https://doi.org/10.1002/joc.6606
37. Guedje FK, Houeto AVV, Houngninou EB et al (2019) Climatology of coastal wind regimes in Benin. Meteorol Z. https://doi.org/10.1127/metz/2019/0930
38. Guijarro JA (2018) Homogenization of climatic series with Climatol. State Meteorol Agency (AEMET), Balear Islands Off Spain
39. Guion A, Turquety S, Polcher J et al (2021) Droughts and heatwaves in the Western Mediterranean: impact on vegetation and wildfires using the coupled WRF-ORCHIDEE regional model (RegIPSL). Clim Dyn. https://doi.org/10.1007/s00382-021-05938-y
40. Hamed KH, Ramachandra Rao A (1998) A modified Mann-Kendall trend test for autocorrelated data. J Hydrol. https://doi.org/10.1016/S0022-1694(97)00125-X
41. Haarsma RJ, Selten F, Hurk B, Vd et al (2009) Drier Mediterranean soils due to greenhouse warming bring easterly winds over summertime central Europe. Geophys Res Lett. https://doi.org/10.1029/2008GL036617
42. Hwang H, Eun SH, Kim BG et al (2020) Occurrence Characteristics of Sea Breeze in the Gangneung Region for 2009–2018. Atmosphere (Basel) https://doi.org/10.14191/ATMOS.2020.30.3.221
43. Jenkinson AF, Collison BP (1977) An initial climatology of gales over the North Sea.Synoptic Climatol. Branch Memo. 62, Met Office, Bracknell, U. K., 18 pp.

44. Jerez S, Montavez JP, Gomez-Navarro JJ et al (2012) The role of the land-surface model for climate change projections over the Iberian Peninsula. J Geophys Res Atmos. https://doi.org/10.1029/2011JD016576
45. Jiang Y, Luo Y, Zhao Z, Tao S (2010) Changes in wind speed over China during 1956-2004. Theor Appl Climatol. https://doi.org/10.1007/s00704-009-0152-7
46. Jones PD, Jonsson T, Wheeler D (1997) Extension to the North Atlantic oscillation using early instrumental pressure observations from Gibraltar and south-west Iceland. Int J Climatol. https://doi.org/10.1002/(sici)1097-0088(19971115)17:13<1433::aid-joc203>3.0.co;2-p
47. Khan B, Abualnaja Y, Al-Subhi AM et al (2018) Climatology of sea breezes along the Red Sea coast of Saudi Arabia. Int J Climatol. https://doi.org/10.1002/joc.5523
48. Kim JC, Paik K (2015) Recent recovery of surface wind speed after decadal decrease: a focus on South Korea. Clim Dyn. https://doi.org/10.1007/s00382-015-2546-9
49. Kusaka H, Kimura F, Hirakuchi H, Mizutori M (2000) The effects of land-use alteration on the sea breeze and daytime heat island in the Tokyo metropolitan area. J Meteorol Soc Japan. https://doi.org/10.2151/jmsj1965.78.4_405
50. Lamb HH (1950) Types and spells of weather around the year in the British Isles: Annual trends, seasonal structure of the year, singularities. Q J R Meteorol Soc. https://doi.org/10.1002/qj.49707633005
51. Laurila TK, Sinclair VA, Gregow H (2021) Climatology, variability, and trends in near-surface wind speeds over the North Atlantic and Europe during 1979–2018 based on ERA5. Int J Climatol. https://doi.org/10.1002/joc.6957
52. Lebassi-Habtezion B, Gonzlez J, Bornstein R (2011) Modeled large-scale warming impacts on summer California coastal-cooling trends. J Geophys Res Atmos. https://doi.org/10.1029/2011JD015759
53. Mahrer Y, Rytwo G (1991) Modelling and measuring evapotranspiration in a daily drip irrigated cotton field. Irrig Sci. https://doi.org/10.1007/BF00190704
54. Martín Vide J, Olcina Cantos J, Madrid (2001) ISBN 84-206-5777-8
55. Martin-Vide J, Lopez-Bustins JA (2006) The Western Mediterranean Oscillation and rainfall in the Iberian Peninsula. Int J Climatol. https://doi.org/10.1002/joc.1388
56. Martinez-Artigas J, Lemus-Canovas M, Lopez-Bustins JA (2021) Precipitation in peninsular Spain: Influence of teleconnection indices and spatial regionalisation. Int J Climatol. https://doi.org/10.1002/joc.6770
57. Masselink G, Pattiaratchi CB (2001) Characteristics of the sea breeze system in Perth, Western Australia, and its effect on the nearshore wave climate. J Coast Res
58. McVicar TR, Roderick ML (2010) Atmospheric science: Winds of change. Nat Geosci. https://doi.org/10.1038/ngeo1002

59. Miao JF, Kroon LJM, Vilà-Guerau de Arellano J, Holtslag AAM (2003) Impacts of topography and land degradation on the sea breeze over eastern Spain. Meteorol Atmos Phys. https://doi.org/10.1007/s00703-002-0579-1
60. Millán MM, Estrela MJ, Miró J (2005) Rainfall components: Variability and spatial distribution in a Mediterranean area (Valencia region). J Clim. https://doi.org/10.1175/JCLI3426.1
61. Millán MM (2014) Extreme hydrometeorological events and climate change predictions in Europe. J Hydrol. https://doi.org/10.1016/j.jhydrol.2013.12.041
62. Miller STK, Keim BD, Talbot RW, Mao H (2003) Sea breeze: Structure, forecasting, and impacts. Rev Geophys. https://doi.org/10.1029/2003RG000124
63. Minola L, Azorin-Molina C, Chen D (2016) Homogenization and assessment of observed near-surface wind speed trends across Sweden, 1956–2013. J Clim. https://doi.org/10.1175/JCLI-D-15-0636.1
64. Minola L, Zhang F, Azorin-Molina C et al (2020) Near-surface mean and gust wind speeds in ERA5 across Sweden: towards an improved gust parametrization. Clim Dyn. https://doi.org/10.1007/s00382-020-05302-6
65. Minola L, Reese H, Lai HW et al (2022) Wind stilling-reversal across Sweden: The impact of land-use and large-scale atmospheric circulation changes. Int J Climatol. https://doi.org/10.1002/joc.7289
66. Misra V, Moeller L, Stefanova L et al (2011) The influence of the Atlantic Warm Pool on the Florida panhandle sea breeze. J Geophys Res Atmos. https://doi.org/10.1029/2010JD015367
67. Morán-Tejeda E, Bazo J, López-Moreno JI et al (2016) Climate trends and variability in Ecuador (1966–2011). Int J Climatol. https://doi.org/10.1002/joc.4597
68. Olcina-Cantos J, Azorin-Molina C (2004) The meteorological importance of sea-breezes in the Levant region of Spain. https://doi.org/10.1256/wea.176.03. Weather
69. Otero N, Sillmann J, Butler T (2018) Assessment of an extended version of the Jenkinson–Collison classification on CMIP5 models over Europe. Clim Dyn. https://doi.org/10.1007/s00382-017-3705-y
70. Palutikof J, Parry M, Smith MS et al (2013) The past, present and future of adaptation: Setting the context and naming the challenges. In: Climate Adaptation Futures. https://doi.org/10.1002/9781118529577.ch1
71. Papanastasiou DK, Melas D, Bartzanas T, Kittas C (2010) Temperature, comfort and pollution levels during heat waves and the role of sea breeze. Int J Biometeorol. https://doi.org/10.1007/s00484-009-0281-9
72. Pastor F, Valiente JA, Estrela MJ (2015) Sea surface temperature and torrential rains in the Valencia region: Modelling the role of recharge areas. Nat Hazards Earth Syst Sci. https://doi.org/10.5194/nhess-15-1677-2015
73. Pausas JG, Millán MM (2019) Greening and Browning in a Climate Change Hotspot: The Mediterranean Basin. Bioscience. https://doi.org/10.1093/biosci/biy157
74. Pazandeh-Masouleh Z, Walker DJ, Crowther JMC (2019) A long-term study of sea-breeze characteristics: A case study of the coastal city of Adelaide. J Appl Meteorol Climatol.

https://doi.org/10.1175/JAMC-D-17-0251.1

75. Perez GMP, Silva Dias MAF (2017) Long-term study of the occurrence and time of passage of sea breeze in São Paulo, 1960–2009. Int J Climatol. https://doi.org/10.1002/joc.5077
76. Qian T, Epifanio CC, Zhang F (2012) Topographic effects on the tropical land and sea breeze. J Atmos Sci. https://doi.org/10.1175/JAS-D-11-011.1
77. Ramis C, Jansà A, Alonso S (1990) Sea breeze in Mallorca. A numerical study. Meteorol Atmos Phys. https://doi.org/10.1007/BF01314828
78. Ramon J, Lledó L, Torralba V et al (2019) What global reanalysis best represents near-surface winds? Q J R Meteorol Soc. https://doi.org/10.1002/qj.3616
79. Real del, Sanchez-Lorenzo A, Lopez-Bustins JA et al (2021) Atmospheric circulation and mortality by unintentional drowning in Spain: from 1999 to 2018. Perspect Public Health. https://doi.org/10.1177/17579139211007181
80. Redaño A, Cruz J, Lorente J (1991) Main features of the sea-breeze in Barcelona. Meteorol Atmos Phys. https://doi.org/10.1007/BF01027342
81. Roderick ML, Rotstayn LD, Farquhar GD, Hobbins MT (2007) On the attribution of changing pan evaporation. Geophys Res Lett. https://doi.org/10.1029/2007GL031166
82. Rojas M, Li LZ, Kanakidou M et al (2013) Winter weather regimes over the Mediterranean region: Their role for the regional climate and projected changes in the twenty-first century. Clim Dyn. https://doi.org/10.1007/s00382-013-1823-8
83. Salvador R, Millán M (2003) Análisis histórico de las brisas en Castellón. Tethys 2:37–51
84. Seager R, Osborn TJ, Kushnir Y et al (2019) Climate variability and change of mediterranean-type climates. J Clim. https://doi.org/10.1175/JCLI-D-18-0472.1
85. Sen PK (1968) Estimates of the Regression Coefficient Based on Kendall's Tau. J Am Stat Assoc. https://doi.org/10.1080/01621459.1968.10480934
86. Shen L, Zhao C, Ma Z et al (2019) Observed decrease of summer sea-land breeze in Shanghai from 1994 to 2014 and its association with urbanization. Atmos Res. https://doi.org/10.1016/j.atmosres.2019.05.007
87. Shen L, Zhao C (2020) Dominance of Shortwave Radiative Heating in the Sea-Land Breeze Amplitude and its Impacts on Atmospheric Visibility in Tokyo, Japan. J Geophys Res Atmos. https://doi.org/10.1029/2019JD031541
88. Shen L, Zhao C, Yang X (2021a) Insight Into the Seasonal Variations of the Sea-Land Breeze in Los Angeles With Respect to the Effects of Solar Radiation and Climate Type. J Geophys Res Atmos. https://doi.org/10.1029/2020JD033197
89. Shen L, Zhao C, Yang X (2021b) Climate-Driven Characteristics of Sea-Land Breezes Over the Globe. Geophys Res Lett. https://doi.org/10.1029/2020GL092308
90. Simpson JE, Mansfield DA, Milford JR (1977) Inland penetration of sea-breeze fronts. Q J R Meteorol Soc. https://doi.org/10.1002/qj.49710343504

91. Simpson JE (1996) Sea breeze and local winds. Cambridge University Press. DOI: 10.2277/0521452112
92. Steele CJ, Dorling SR, Von Glasow R, Bacon J (2015) Modelling sea-breeze climatologies and interactions on coasts in the southern North Sea: Implications for offshore wind energy. Q J R Meteorol Soc. https://doi.org/10.1002/qj.2484
93. Sydeman WJ, García-Reyes M, Schoeman DS et al (2014) Climate change and wind intensification in coastal upwelling ecosystems. Science 80. https://doi.org/10.1126/science.1251635
94. Tetzner D, Thomas E, Allen C (2019) A validation of ERA5 reanalysis data in the southern antarctic peninsula—Ellsworth land region, and its implications for ice core studies. https://doi.org/10.3390/geosciences9070289. Geosci
95. Theil H (1950) A rank-invariant method of linear and polynomial regression analysis, Part I. Proc. R. Netherlands Acad. Sci
96. Tierney JE, Pausata FSR, De Menocal PB (2017) Rainfall regimes of the Green Sahara. Sci Adv. https://doi.org/10.1126/sciadv.1601503
97. Troccoli A, Muller K, Coppin P et al (2012) Long-term wind speed trends over Australia. J Clim. https://doi.org/10.1175/2011JCLI4198.1
98. Tuel A, Eltahir EAB (2020) Why Is the Mediterranean a Climate Change Hot Spot? J Clim. https://doi.org/10.1175/JCLI-D-19-0910.1
99. Vahmani P, Ban-Weiss G (2016a) Climatic consequences of adopting drought-tolerant vegetation over Los Angeles as a response to California drought. Geophys Res Lett. https://doi.org/10.1002/2016GL069658
100. Vahmani P, Sun F, Hall A, Ban-Weiss G (2016b) Investigating the climate impacts of urbanization and the potential for cool roofs to counter future climate change in Southern California. Environ Res Lett. https://doi.org/10.1088/1748-9326/11/12/124027
101. Vautard R, Cattiaux J, Yiou P et al (2010) Northern Hemisphere atmospheric stilling partly attributed to an increase in surface roughness. Nat Geosci. https://doi.org/10.1038/ngeo979
102. Vautard R, Van Jan G, Otto FEL et al (2019) Human influence on European winter wind storms such as those of January 2018. Earth Syst Dyn. https://doi.org/10.5194/esd-10-271-2019
103. Wu J, Zha J, Zhao D, Yang Q (2018) Changes in terrestrial near-surface wind speed and their possible causes: an overview. Clim Dyn. https://doi.org/10.1007/s00382-017-3997-y
104. Xu M, Chang CP, Fu C et al (2006) Steady decline of east Asian monsoon winds, 1969–2000: Evidence from direct ground measurements of wind speed. J Geophys Res Atmos. https://doi.org/10.1029/2006JD007337
105. Young IR, Ribal A (2019) Multiplatform evaluation of global trends in wind speed and wave height. Science 80. https://doi.org/10.1126/science.aav9527
106. Zappa G, Hawcroft MK, Shaffrey L et al (2015) Extratropical cyclones and the projected decline of winter Mediterranean precipitation in the CMIP5 models. Clim Dyn. https://doi.org/10.1007/s00382-

014-2426-8

107. Zecchetto S, De Biasio F (2007) Sea surface winds over the Mediterranean basin from satellite data (2000-04): Meso- and local-scale features on annual and seasonal time scales. J Appl Meteorol Climatol. https://doi.org/10.1175/JAM2498.1
108. Zeng Z, Ziegler AD, Searchinger T et al (2019) A reversal in global terrestrial stilling and its implications for wind energy production. Nat Clim Chang. https://doi.org/10.1038/s41558-019-0622-6
109. Zha J, Shen C, Li Z et al (2021) Projected changes in global terrestrial near-surface wind speed in 1.5 °c-4.0 °c global warming levels. Environ Res Lett. https://doi.org/10.1088/1748-9326/ac2fdd
110. Zhang X, Lu C, Guan Z (2012) Weakened cyclones, intensified anticyclones and recent extreme cold winter weather events in Eurasia. Environ Res Lett. https://doi.org/10.1088/1748-9326/7/4/044044
111. Zhang G, Azorin-Molina C, Chen D et al (2020) Variability of daily maximum wind speed across China, 1975–2016: An examination of likely causes. J Clim. https://doi.org/10.1175/JCLI-D-19-0603.1
112. Zhang N, Wang Y (2021) Mechanisms for the isolated convections triggered by the sea breeze front and the urban heat Island. Meteorol Atmos Phys. https://doi.org/10.1007/s00703-021-00800-6
113. Zhu M, Atkinson BW (2004) Observed and modelled climatology of the land-sea breeze circulation over the Persian Gulf. Int J Climatol. https://doi.org/10.1002/joc.1045
114. Zhu L, Meng Z, Zhang F, Markowski PM (2017) The influence of sea- and land-breeze circulations on the diurnal variability in precipitation over a tropical island. Atmos Chem Phys. https://doi.org/10.5194/acp-17-13213-2017

Figures

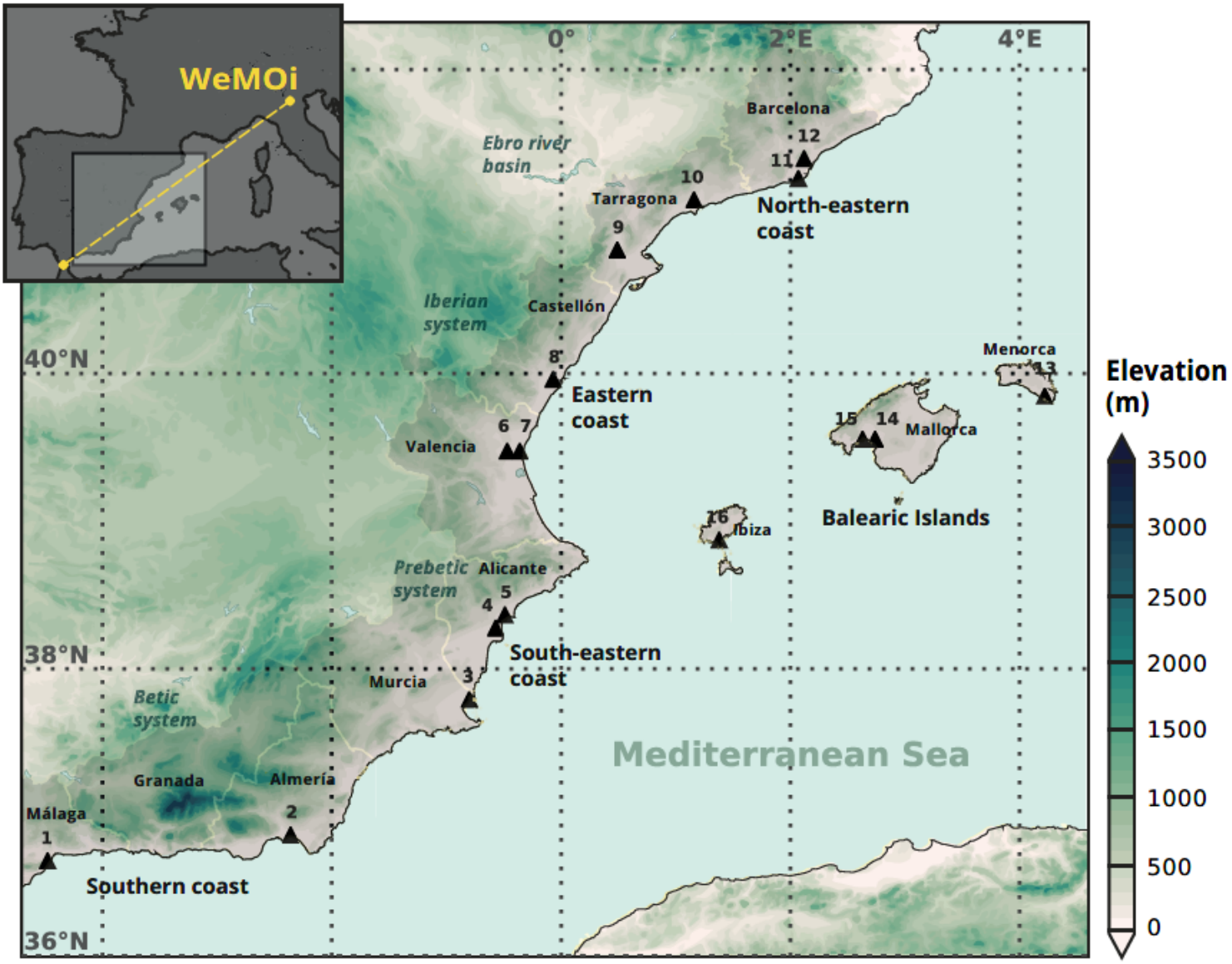

Figure 1

Terrain map of the Eastern Spain with location of the 16 weather stations (triangles), the numbers and limits of each region are detailed in Tables 1 and 2. The inset upper left picture shows the transect of the WeMOI used to detect SB events.

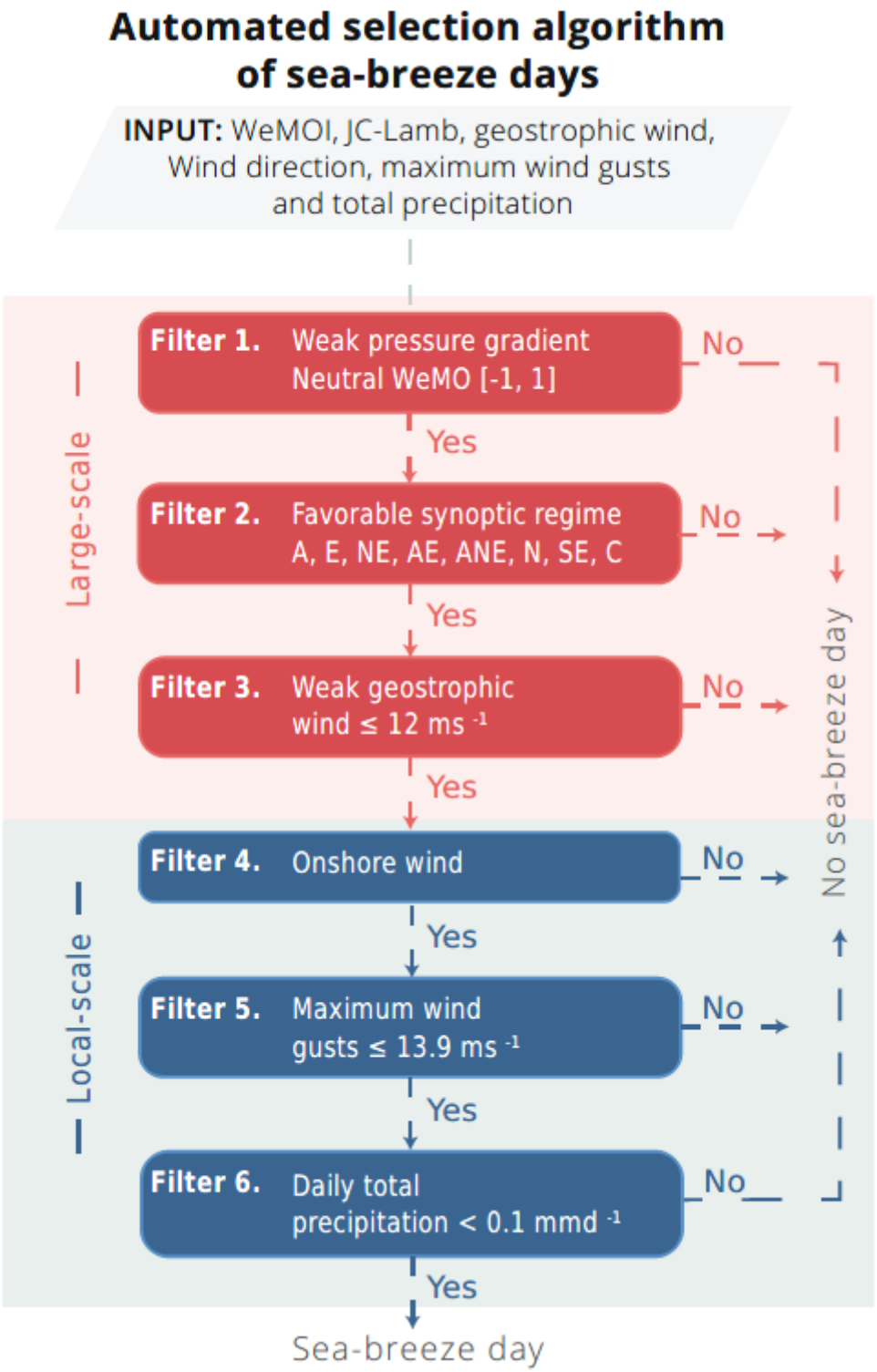

Figure 2

Workflow diagram of the SB automated selection algorithm.

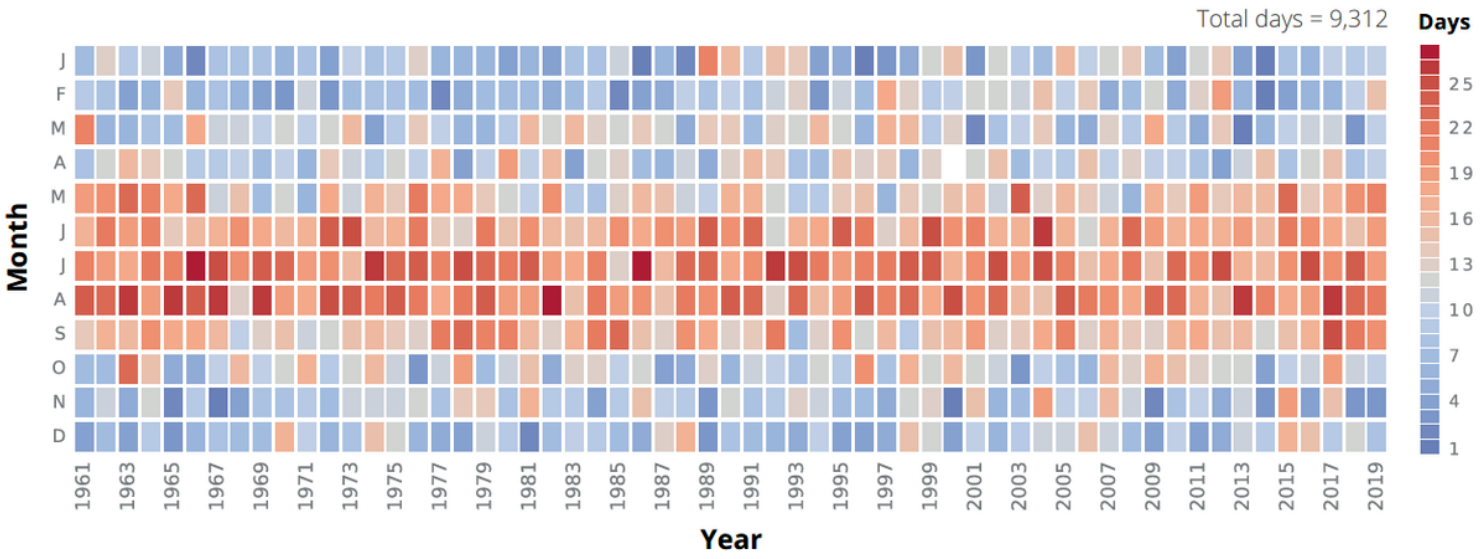

Figure 3

Total number of SB days identified across all weather stations (regional level) in every month and year for 1961–2019.

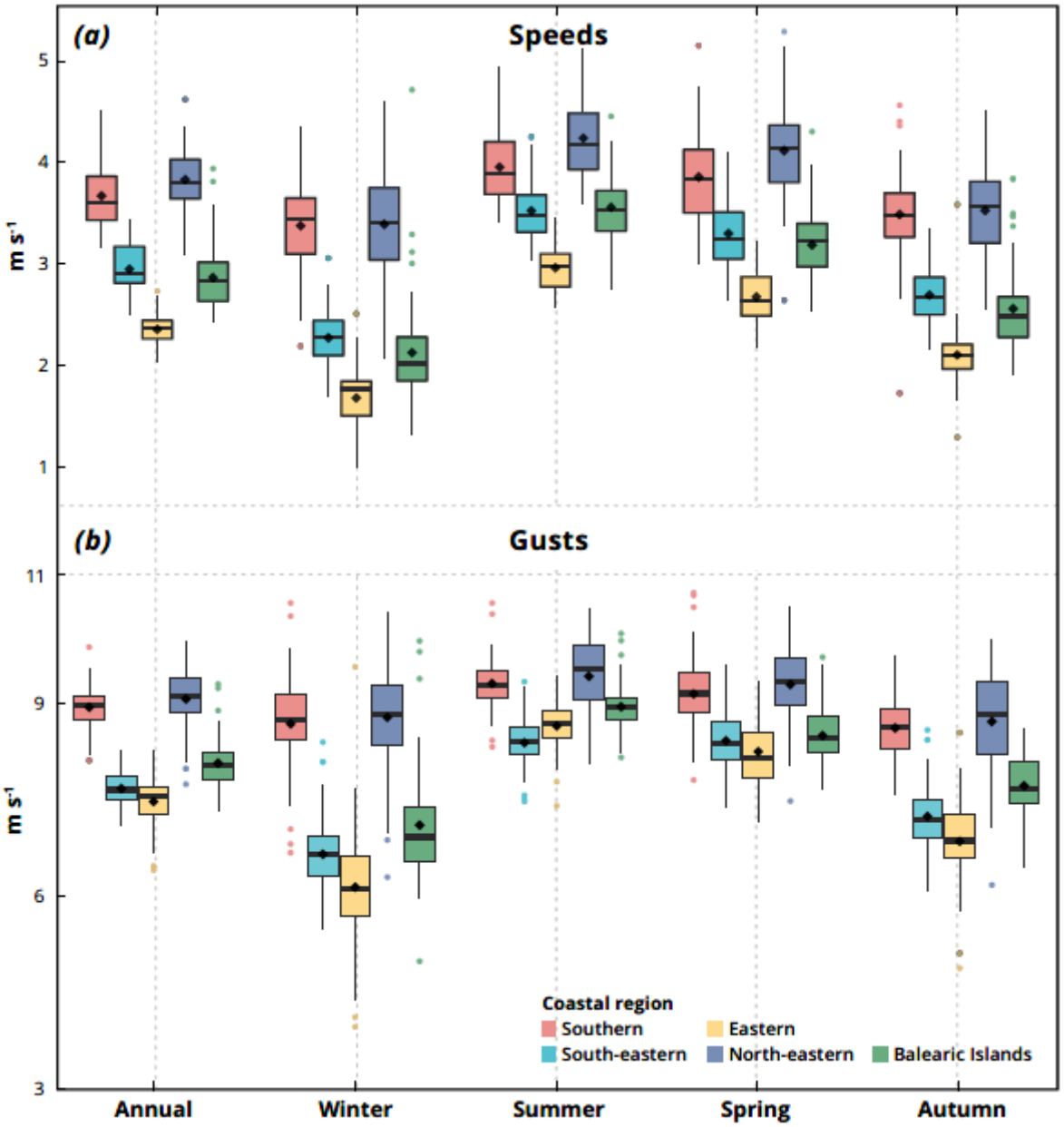

Figure 4

Annual and seasonal box and whisker plot of SB speeds (a) and gusts (b) for each coastal region for 1961–2019. The mean is represented with a black dot, while the median with a black line. The boxes describe the 25th and 75th percentile range, while the whiskers exhibit the 10th and 90th percentiles. Outlier values are presented with colored dots.

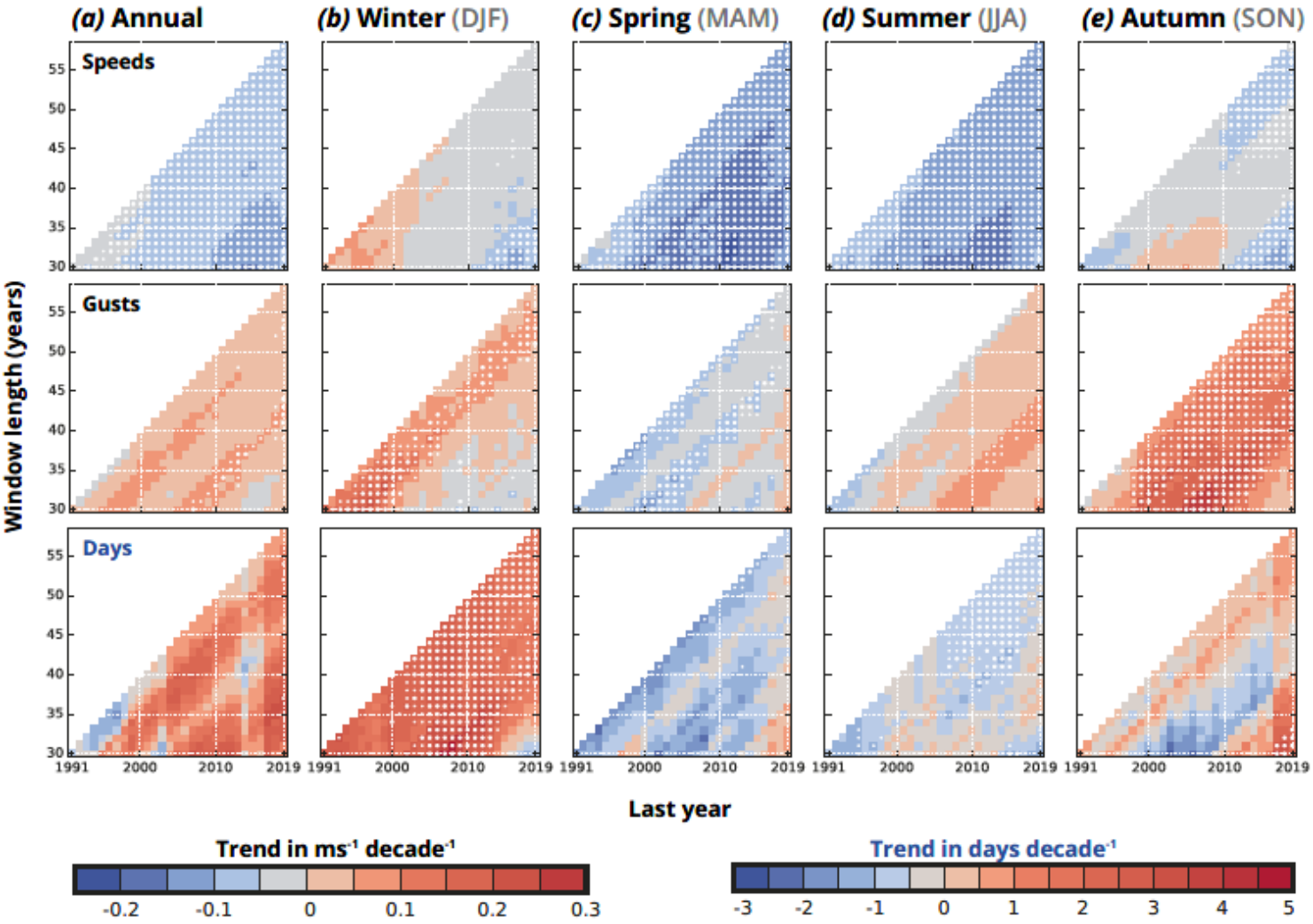

Figure 5

Regional running trends of total SB days (in days decade^{-1}), SB speeds and gusts (in ms^{-1} decade^{-1}) obtained from weighted average over all 16 stations across Eastern Spain for 1961–2019. White dots represent trends significance at $p < 0.10$ (small ones) and $p < 0.05$ (bigger ones). Coastal level running trends are shown in the supplemental material (Fig. S4-S5).

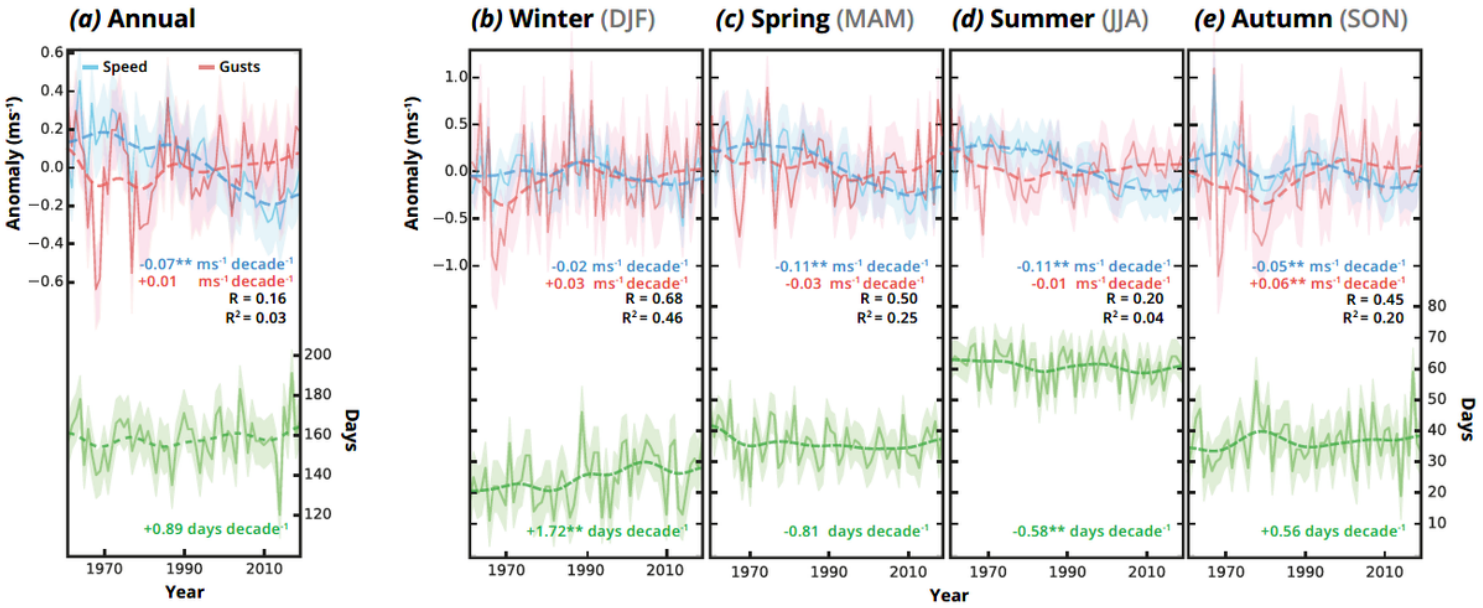

Figure 7

Regional variability (weighted) for the SB speeds (blue), gusts (red) and occurrence (green) across Eastern Spain for 1961–2019. The 15-years Gaussian low-pass filter (dashed line) is also shown, while the shaded area represents the standard deviation. Trends for the 58-year period are indicated with their statistical significance, i.e., $p < 0.10$ (one asterisk) and $p < 0.05$ (two asterisks), while Pearson correlation coefficient (r) and coefficient of determination (R^2) between the SB speeds and gusts are also shown.

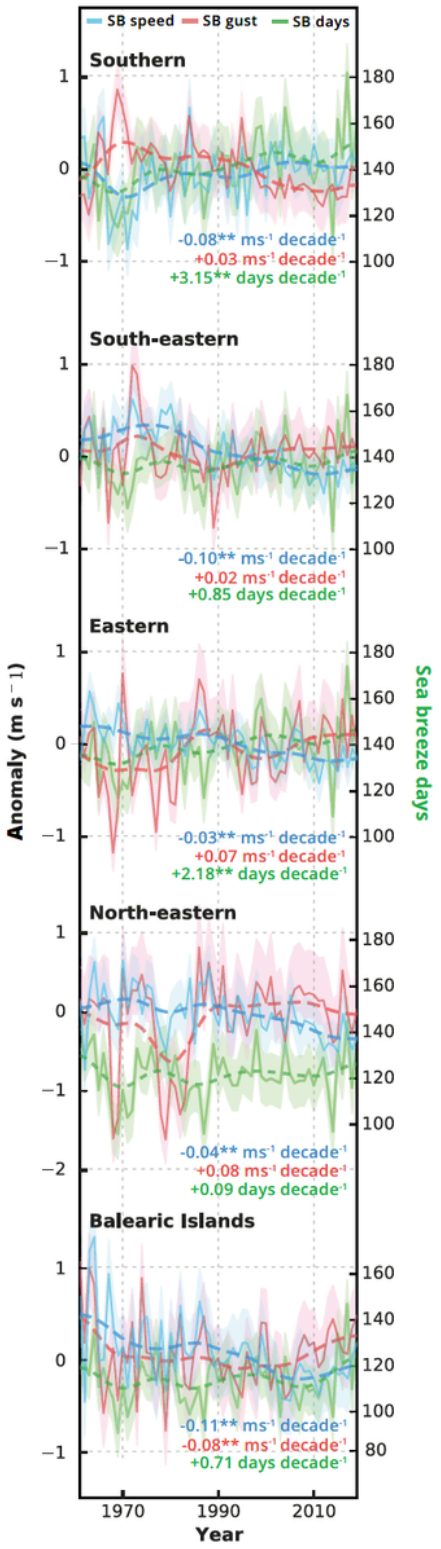

Figure 8

Annual variability (weighted) for the SB speeds (blue), gusts (red) and occurrence (green) for each coastal region over the Eastern Spain for 1961-2019. The 15-years Gaussian low-pass filter (dashed line) is also shown. Trends for the 58-year period are indicated with their statistical significance, i.e., $p < 0.10$ (one asterisk) and $p < 0.05$ (two asterisks). Seasonal variability is displayed in the supplemental material (Fig. S8).

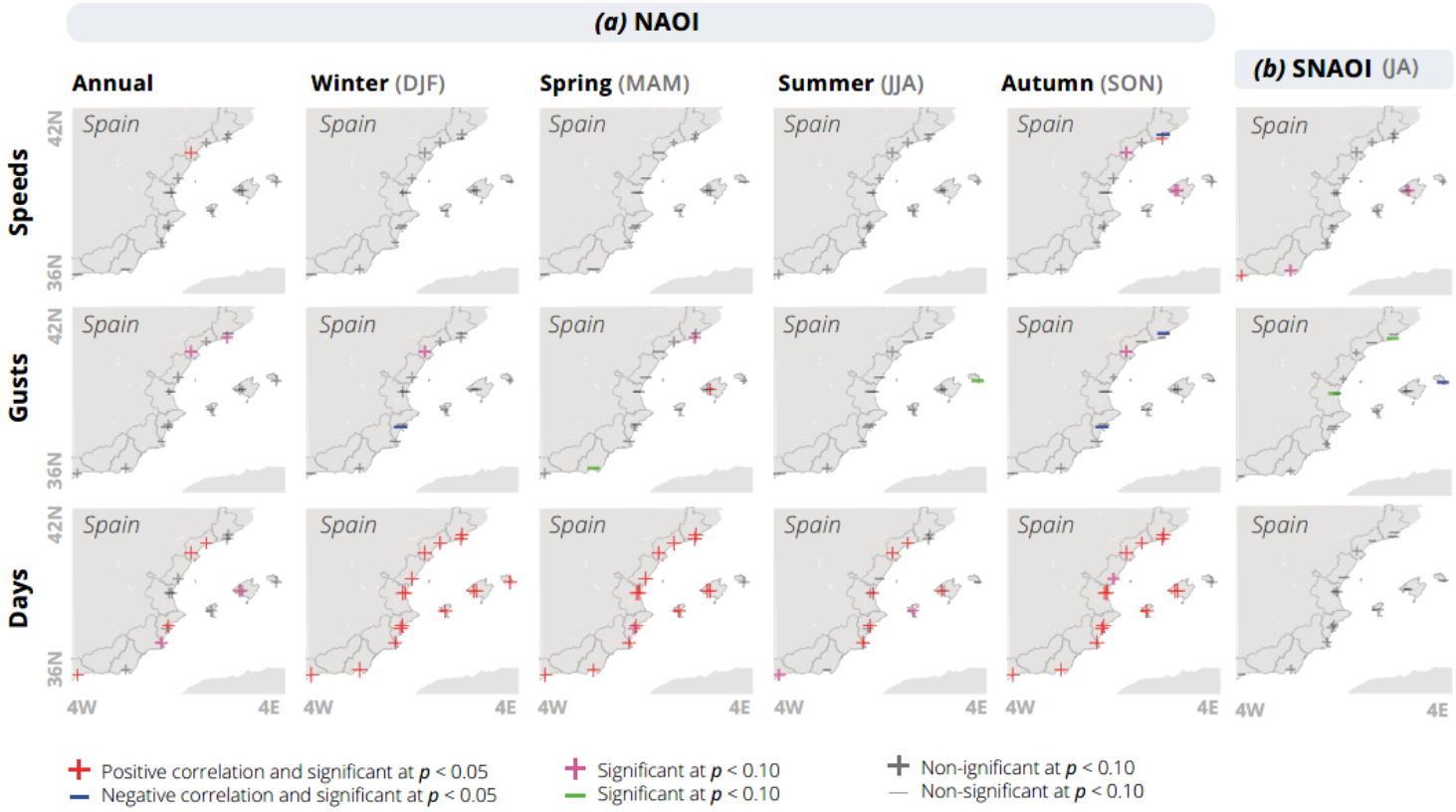

Figure 9

Spatial distribution of the sign and significance of Pearson's correlation relationship (r) between the SB speeds and the SB gusts anomalies (m s^{-1}), the SB days and the (a) NAOI and (b) SNAOI for 16 stations in Eastern Spain for 1961–2019. Markers (plus and minus) indicate the sign of the relationship while colors represent the statistical significance at $p < 0.05$ (blue and red), $p < 0.10$ (green and magenta), and $p > 0.10$ (gray). Pearson's correlation coefficients for the regional and coastal series are presented in Tables 5-7.

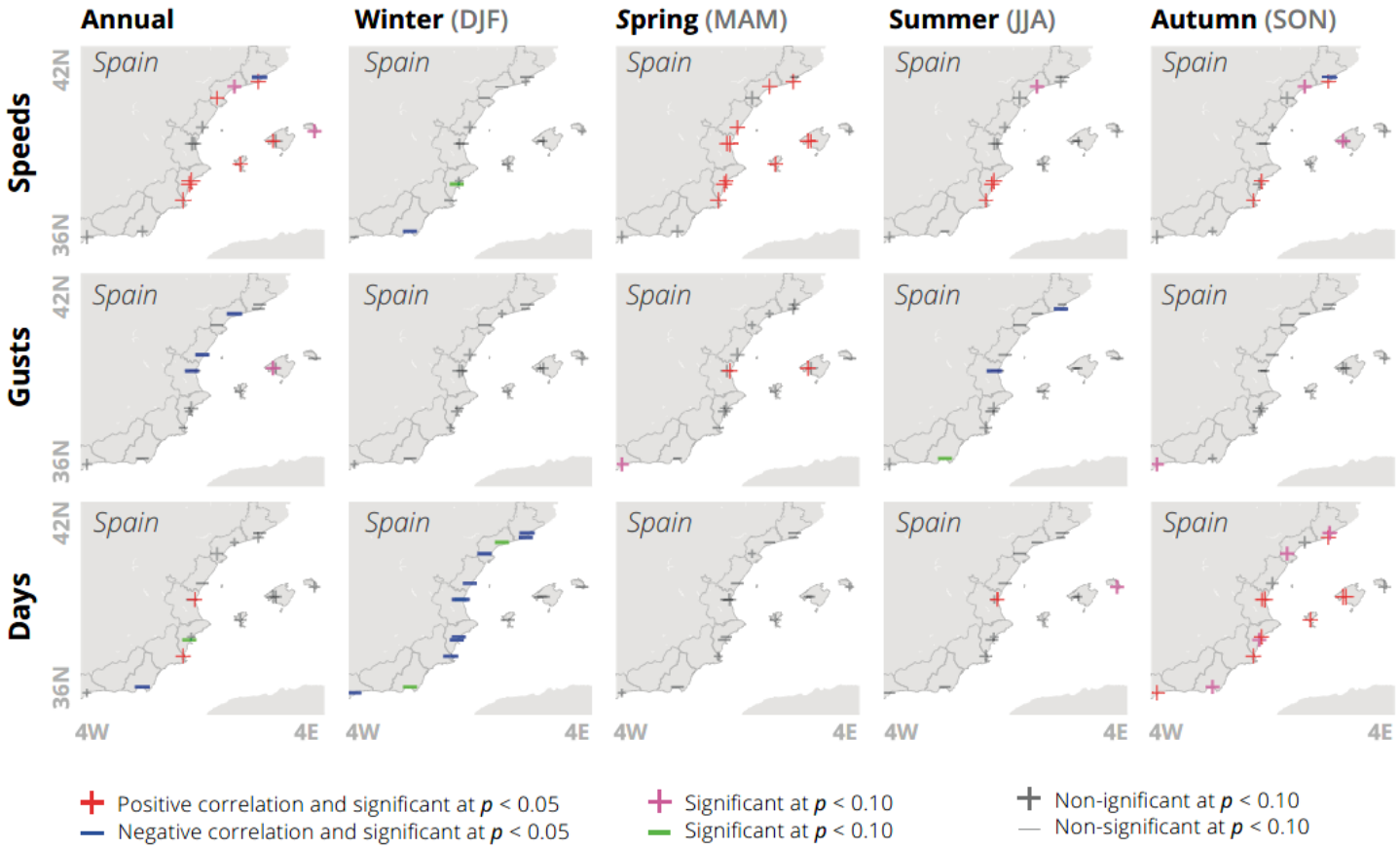

Figure 10

As Fig. 9 but for the WeMOI.

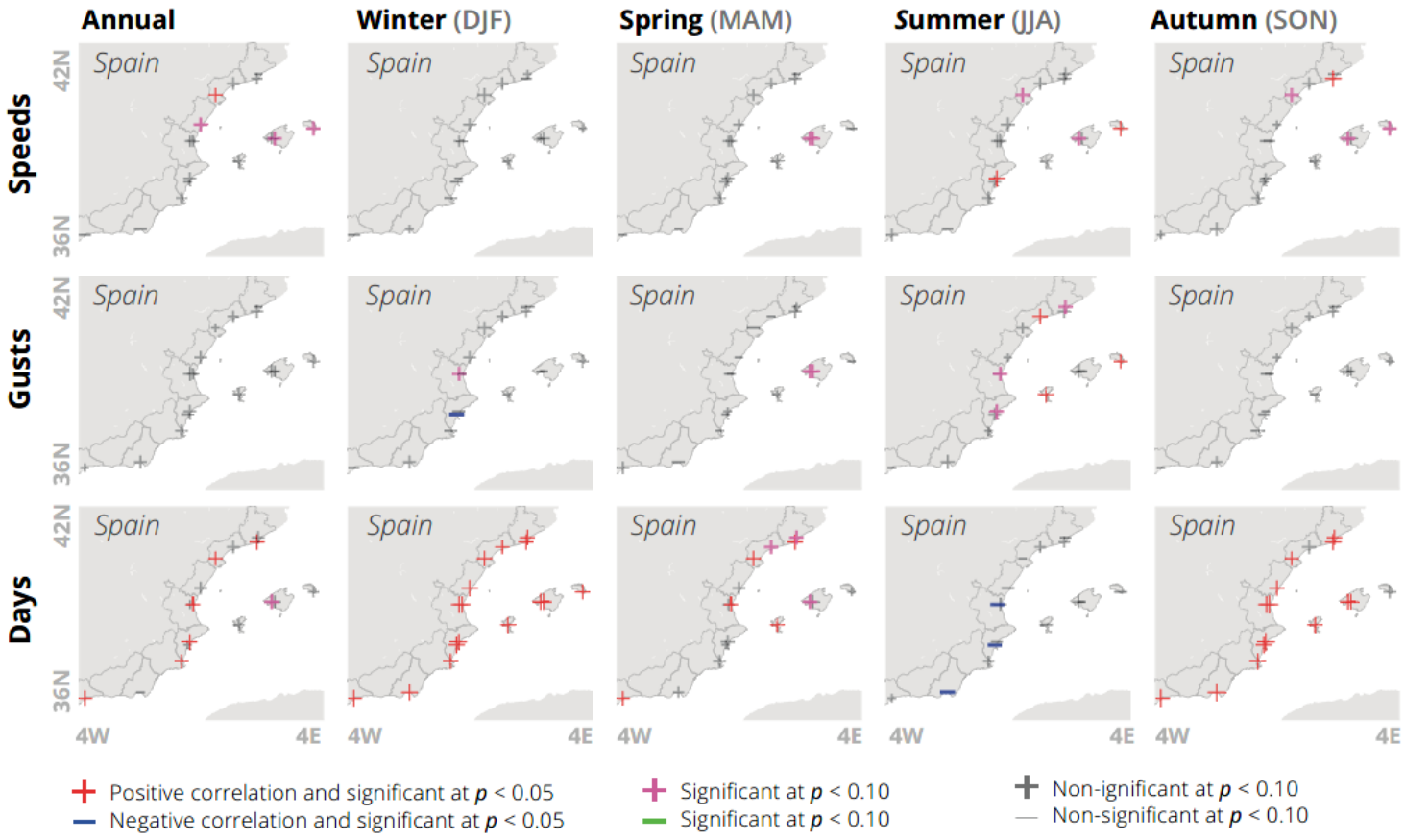

Figure 11

As Fig. 9 but for the MOI.

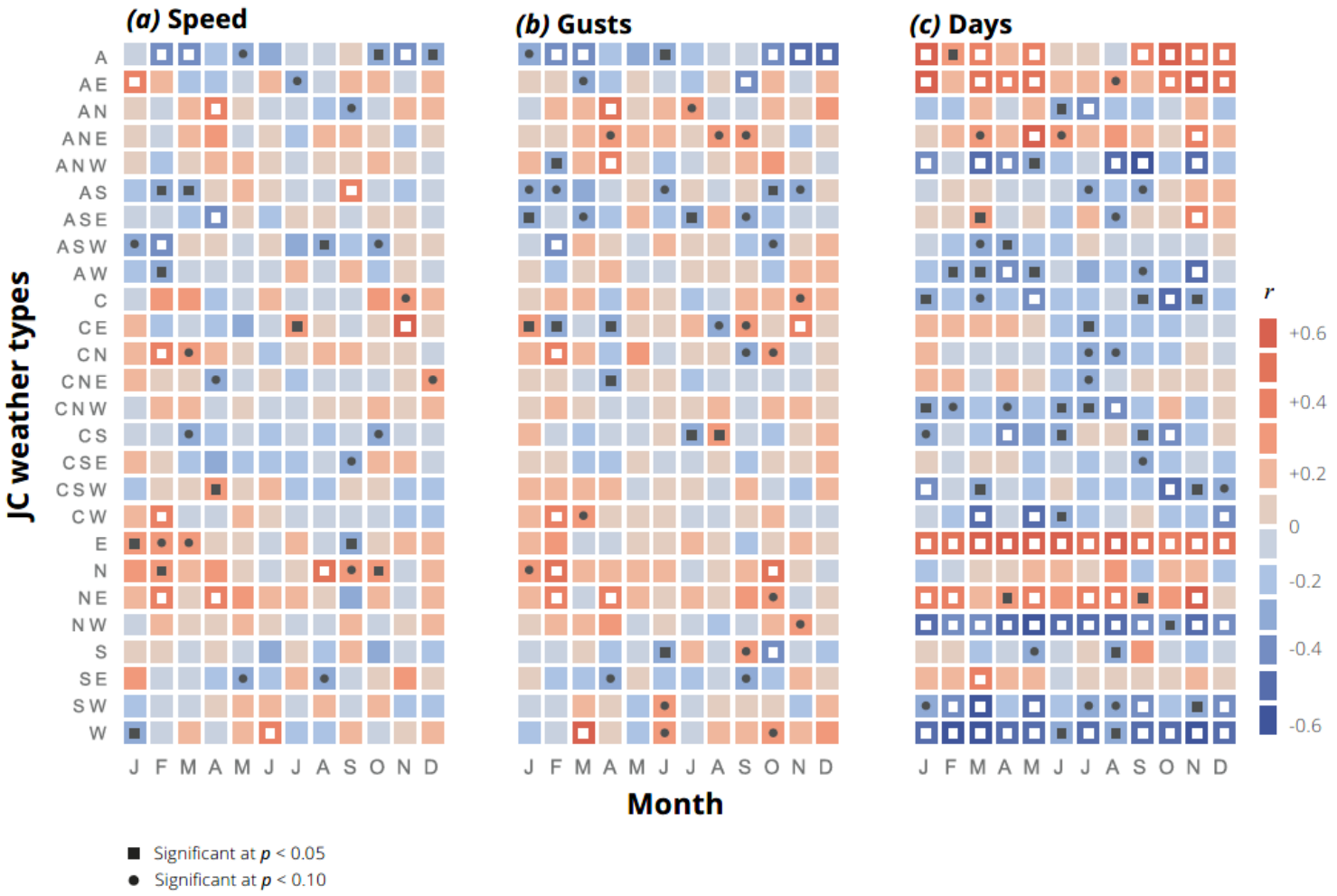

Figure 12

Monthly Pearson's correlation coefficients (*r*) between the SB (a) speeds, (b) gusts and (c) occurrence, and the 26 Jenkinson and Collison's (JC) weather types for 1961–2019. Squares mask the *r* significance at $p < 0.05$, and circles at $p < 0.10$. Bar colors refer to *r* magnitude and sign. Coastal-based relationships between JC types and SB were also explored in supplemental material (Fig. S10-S14).

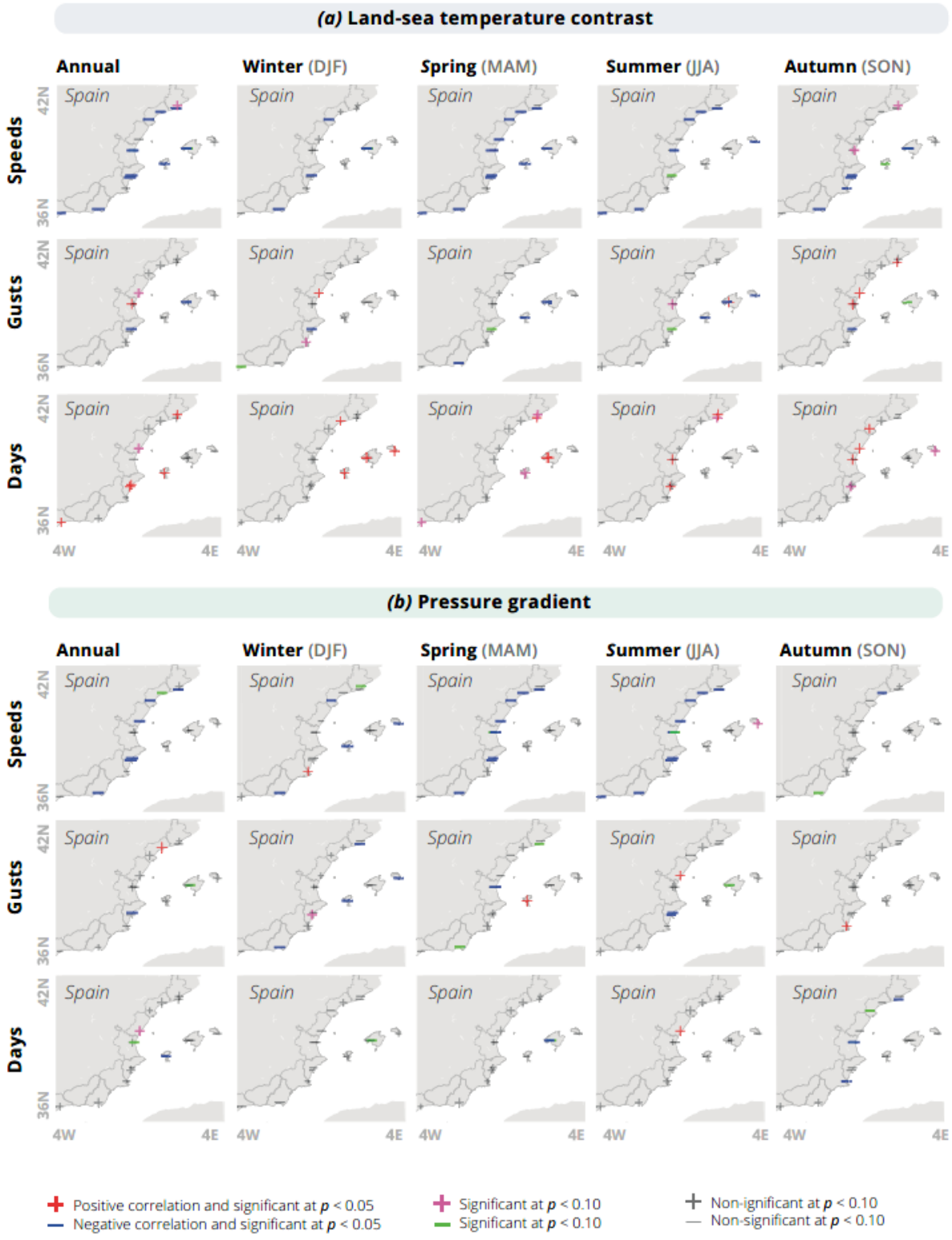

Figure 13

As Fig. 9 but for (a) land-sea temperature difference and (b) horizontal pressure gradient.

Supplementary Files

This is a list of supplementary files associated with this preprint. Click to download.

- SupplementalFigures.pdf